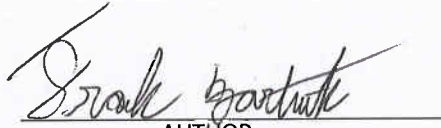APPROVAL SHEET

The thesis

is submitted in partial fulfillment of the requirements

for the degree of

Master of Science

_____
AUTHOR

The thesis has been read and approved by the examining committee:

_____
Advisor

_____

_____

_____

_____

_____

Accepted for the School of Engineering and Applied Science:

_____

Dean, School of Engineering and Applied Science

May

2013

Purification of Recombinant Polyclonal Antibodies by Ion Exchange Chromatography

---

A Thesis

Presented to

the faculty of the School of Engineering and Applied Science

University of Virginia

In partial Fulfillment

of the requirements for the Degree

Master of Science in Chemical Engineering

by

Frank Bartnik

February 2013

Abstract

The equilibrium parameters and transport kinetics of three monoclonal antibodies (mAbs) and antibody aggregates were investigated as a model to determine suitable operating conditions for the purification of a new class of bio-therapeutics known as recombinant polyclonal antibodies. Three process-scale strong cation exchangers, UNOsphere Rapid S, POROS 50HS and Nuvia S were examined; the former two are macroporous rigid particles, whereas the latter contains dextran grafts inside the pores. The effects of counterion type and pH on retention were also examined.

The mAb effective diffusivity was determined for each resin under both non-binding and gradient elution conditions. Non-binding conditions results showed that pore diffusion was dominant for UNOsphere Rapid S and POROS 50HS but that complete exclusion from the pores occurred for Nuvia S. However, under gradient elution conditions, the effective diffusivity was approximately the same for each resin.

A procedure was developed to generate soluble aggregates from one of the mAbs and the aggregate retention characteristics were determined. The size of the aggregates was estimated using size exclusion chromatography and dynamic light scattering. The results showed that the aggregates formed were in the size range expected, dimers and tetramers. The aggregate ion exchange equilibrium parameters were then determined on POROS 50HS and Nuvia S. Using the retention factors for the single component mAbs as well as the mAb aggregates, a step elution scheme was devised to separate the aggregates without resolving the individual mAbs.

Acknowledgements

Table of Contents

List of Figures

List of Tables

List of Symbols

A affinity parameter in mass action law model

Bi Biot Number

C protein concentration in the bulk liquid (mg/mL)

C_i liquid phase concentration of component i (mol/L) or (mg/mL)

C_o initial protein concentration

C_s protein concentration at the particle surface (mg/mL)

CV   number of column volumes of mobile phase passed

d_P particle diameter (μm)

D_e effective pore diffusivity (cm^2/s)

D_o protein diffusivity in free solution (cm^2/s)

D_s protein diffusivity in the absorbed state (cm^2/s)

h reduced height equivalent to a theoretical plate

H height equivalent to a theoretical plate (cm)

J transfer flux

k_f film mass transfer coefficient

k' protein retention factor

k'_M protein retention factor under non-binding conditions

$K_{i,j}$ ion exchange equilibrium constant

L column length (cm)

q_i concentration in adsorbed phase (mol/L) or (mg/mL)

q_o charge density (mol/L)

r_h hydrodynamic radius (nm)

r_p particle radius (μm)

Sh Sherwood number

v mobile phase velocity (cm/s)

v' reduced velocity

V_c column volume (mL)

V_R retention volume of a component (mL)

W baseline peak width (mL)

z_i effective charge of component, i

Greek Symbols

β gradient slope

ε extraparticle porosity

ε_p intraparticle porosity

γ normalized gradient slope

σ steric hindrance factor

τ_p tortuosity factor

ψ_p hindrance parameter

ϕ column void fraction

1. Introduction

The production of biological drugs has increased rapidly in recent years, placing a greater demand for process understanding and optimized designs. Downstream purification is often the biggest obstacle in the production of these molecules due to the physical and technological constraints of large-scale chromatography columns. With a constantly growing number of different biological products, new process complexities have arisen, requiring new purification techniques and models.

Ion exchange chromatography (IEC) is the most widely employed industrial scale purification technique for bio-therapeutics. There are two types of ion exchange chromatography, cation exchange chromatography, which uses a negatively charged matrix to reversibly bind positively charged proteins, and anion exchange chromatography, which uses a positively charged matrix to reversibly bind negatively charged proteins.

Ion exchangers are often employed in two types of downstream processing steps; "capture", where the product of interest is bound while many unrelated impurities pass through the column and "purification", where product related impurities are separated from the product of interest. Ion exchange chromatography is also used in "polishing" steps to remove trace amounts of adventitious agents.

Generally, mAb purification follows a basic processing scheme a protein A chromatography capture step, followed by an anion exchange chromatography flow through step, a cation exchange chromatography purification step, and a polishing step. Protein A is a highly selective immunoglobulin-binding protein that has been engineered and attached to the surface of a chromatography matrix. Protein A selectively and strongly binds human IgG at neutral pHs.

Most of the other species in the supernatant, such as host cell proteins, DNA, and viruses are not bound by protein A and flow through the column. However, some of these impurities will bind to the chromatographic matrix itself and will often elute under the same low pH conditions required to elute a mAb from protein A (Shukla and Hinckley, 2008). Additionally, the eluting conditions required by protein A chromatography often create product-related impurities, such as mAb aggregates, as these proteins have a tendency to irreversibly aggregate at low pHs (Ejima et al., 2007).

After eluting from the protein A column, the mAb eluate flows through an anion exchange column, designed to capture acidic impurities remaining in the supernatant, often the remaining DNA and host cell proteins, while allowing for the IgG and IgG-like impurities to flow through.

The next step in the chromatographic purification of mAbs is a cation exchange step. This is often the most difficult separation because mAb aggregates, especially dimers, have retention properties similar to those of the mAbs product. With such similarity between product and impurity, this process is very sensitive and must be carefully designed.

Although mAbs can be effective in treating a variety of ailments from cancer to autoimmune diseases to specific infections, their high selectivity limits their ability to combat the most complex infectious agents and to target epitopes with multiple variants (Frandsen et al., 2011). In order to treat these diseases, a new class of bio-therapeutics has been proposed, known as recombinant polyclonal antibodies (rpAbs). Consisting of a well-defined and characterized mixture of mAbs, rpAbs could provide the same or even greater potency of mAbs while also allowing for a broader spectrum and greater therapeutic efficiency.

Under current Food and Drug Administration regulations, it appears advantageous to design rpAb purification processes that are capable of removing undwanted impurities without separting the individual antibody components (FDA, 2004). In this case, it may be possible to treat the rpAb mixture as a single drug product avoiding the common requirement of clinical testing of each component for mixed drugs. Recent studies by Bregenholt et al. (2006) and Frandsen et al. (2011) have shown the ability to consistenly produce rpAbs in a single polyclonal cell bank. The next obstacle is the purification without separation of the antibody components from each other. This is straightforward for protein A and flow-through step but not immediately obvious for aggregate clearance.

In this work, we thus focus on the separation of monoclonal antibody aggregates from a mixture of three monoclonal antibodies by cation exchange chromatography. The specific aims of this work are to:

a. Determine the chromatographic properties of the three mAbs individually, using different buffer types, pHs, counter-ions, and resins.

b. Characterize the low pH aggregation of a single mAb as well as the aggregates chromatographic behavior.

c. Separate aggregates from antibodies based on the single component mAb properties in combination with the aggregate properties.

d. Determine suitable operating conditions for rpAb elution based on the single component behavior.

Tools used to address these aims include:

a. Iso-electric focusing to determine the iso electric point (pI) of each individual monoclonal antibody.

b. Ion exchange chromatography (IEC) operated with a linear gradient to determine the retention properties of each individual mAb as well as the aggregates.

c. Size exclusion chromatography (SEC) and dynamic light scattering (DLS) to determine the size of the aggregates produced.

The results of this research are expected to not only provide a basis for a model for the purification of recombinant polyclonal antibodies based, but also understanding of the chromatographic behavior of mAb aggregates.

2. Background

This section provides theoretical background for two critical aspects of this work, (a) ion exchange equilibrium and (b) protein transport.

2.1 Ion Exchange Equilibrium Theory

The mass action (MA) model provides the basic frame work to describe ion exchange equilibrium (Helfferich, 1962). This model describes the exchange of a counterion A with charge z_A with another counterion B with charge z_B by the following equation:

$$K_{A,B} = \frac{q_A (C_B)^{z_A/z_B}}{C_A (q_B)^{z_A/z_B}}$$

(2.1)

subject to the charge balance conditions:

$$q_o = z_A q_A + z_B q_B$$

(2.2)

$$C_o = z_A C_A + z_B C_B$$

(2.3)

where $K_{A,B}$ is an equilibrium constant, q_o is the exchanger charge density, and C_o is the equivalent co-ion concentration. This model works well for the exchange of small counterions but often fails to describe the exchange of proteins. There are two distinct causes for this failure. First, proteins the charge z_A is generally different from their net charge and therefore z_A is denoted as the effective charge as it depends on the heterogeneous distribution of charges on the protein surface (Brooks and Cramer, 1992; Yamamoto et. al., 1988). This is not known a priori and, thus, must be determined empirically. Secondly, upon binding protein molecules can block a number of the charged ligand groups making them unavailable for ion exchange. As a result, the

effective ion exchange charge density varies with protein load. While the latter is a concern only at high protein loads, the former is always true.

The Steric Mass Action (SMA) model was developed by Brooks and Cramer (199) to describe the exchange of a protein and a small counter-ion on the ligand functional group taking into account these two factors. This model incorporates a steric hindrance factor, which takes into account resin ligands which are shielded by the bound protein. Accordingly, eq. 2.2 is replaced by:

$$q_o = (z_P + \sigma_P)q_P + z_B q_B \tag{2.4}$$

where p is the protein and σ_P is the number of surface ligands blocked or shielded by one bound protein. Combining eqs. 2.1 and 2.4 yields:

$$K_{P,B} = \frac{q_P (z_B C_B)^{z_P/z_B}}{C_P \left[q_o - (z_P + \sigma_P) q_P \right]^{z_B/z_P}} \tag{2.5}$$

where q_o is the charge density, q_P and C_B are the adsorbed and liquid phase protein concentrations, respectively, C_B is the counter-concentration (normally assumed to be equal to C_o because the protein is usually present in small molar concentrations), z_P is the effective protein charge, and $K_{P,B}$ is the adsorption equilibrium constant for the exchange of the protein and counter-ion. At low protein loads, eq 2.6 reduces to:

$$q_P = K_{P,B} \left(\frac{q_o}{z_B C_B} \right)^{z_P/z_B} C_P = m C_P \tag{2.6}$$

where $m = K_{P,B}(q_o/z_B C_B)^{z_P/z_B} C_P$. Taking into account retention in particle pores, this equation can also be used to relate the protein retention factor, k', to the salt concentration according to the following equation

$$k' = k'_M + \phi m \qquad (2.7)$$

where $\phi = (1-\varepsilon)/\varepsilon$. Accordingly,

$$k' = k'_M + A C_B^{-z_P/z_B} \qquad (2.8)$$

where k'_M is the retention factor obtained for non-binding conditions (i.e. $C_B \rightarrow \infty$) and $A = \phi K_{P,B}(q_o / z_B)^{z_P/z_B}$ (Carta and Jungbauer, 2010).

2.2 Protein transport in ion exchange media

Protein transport within the particles is typically the rate-limiting step (Carta and Jungbauer, 2010). Therefore, understanding mass transfer rates and mechanisms is important (Carta et. al, 2005)

Diffusional mass transfer often controls protein adsorption kinetics because proteins are large and, thus, have low diffusivities. Both extra and intraparticle transport can affect the adsorption of proteins, however their individual contributions are different under different conditions and different mechanisms.

2.2.2 Intraparticle transport

In general, diffusion-limited transport of proteins can occur through many different mechanisms including, "pore diffusion", "surface diffusion", or combination of both (LeVan and

Carta, 2007). The driving force for pore diffusion is a concentration gradient in the solution contained within the pores. The flux is therefore defined by:

$$J = -D_e \nabla C_P \tag{2.9}$$

where D_e is the effective pore diffusivity and C_p is the protein concentration in solution. Pore diffusion has been observed as the dominant mechanism of transport in macroporous resins (Tao et al., 2011; Weaver and Carta, 1996). The following equation has been shown to provide an estimate of the effective pore diffusivity in macroporous resins:

$$D_e \sim \frac{\psi_p \varepsilon_p D_0}{\tau_p} \tag{2.10}$$

where D_o is the free solution diffusivity, ψ_p is a diffusional hindrance factor, ε_p the intraparticle porosity, and τ_P the tortuosity factor (Carta and Jungbauer, 2010). ψ_p accounts for hindered diffusion effects and depends on the ratio of protein and pore size, ε_p accounts for the fact that pore diffusion can only occur through the open pore area and τ_P accounts for the fact that the pores are not straight paths, thus making the actual diffusion path longer. Since ψ_p and ε_p are less than 1 and τ_P is greater than one, the ratio D_e/D_o is always less than one for pore diffusion.

The mechanism of surface diffusion relies on a gradient in the absorbed phase concentration to drive transport. The flux for this case is represented by (LeVan and Carta, 2007):

$$J = -D_s \nabla q \tag{2.11}$$

where D_s is the protein diffusivity in the adsorbed state and q is the adsorbed phase protein concentration. In this case, it is believed that proteins move by either sliding along the surface of the matrix, or by "hopping" from site to site on the matrix without escaping the electrostatic interaction with the charge surface groups. This behavior has been observed to enhance the mass transfer of proteins in matrices which contain charged surface extenders, such as Nuvia S (Perez Almodovar, et al., 2012).

2.2.1 Extraparticle transport

Extraparticle transport is described in terms of a boundary layer resistance to mass transfer and is represented by a mass transfer coefficient, k_f. The mass transfer flux of a protein is therefore defined by the following equation (LeVan and Carta, 2007):

$$J = k_f \left(C - C_s \right) \qquad (2.12)$$

where J is the flux, C is the bulk protein concentration and C_s is the protein concentration at the particle surface. k_f is usually expressed by the Sherwood number, $Sh=k_f d_p/D_o$, where d_p is the particle diameter and D_o is the free solution diffusivity (Cussler, 1997). The value of the Sherwood number is determined by the flow outside of the particles caused by a pressure gradient inside of a packed column.

2.2.3 Comparison of extraparticle and intraparticle resistance

As previously stated, both intraparticle and extraparticle resistances can affect the overall rate of transport. The relative importance of each can be described by the Biot number, Bi, defined as follows:

$$Bi = \frac{k_f r_p}{D_e} \qquad (2.13)$$

or

$$Bi = \frac{1}{2} \frac{Sh}{D_e / D_o} \qquad (2.14)$$

where r_p is the particle radius. In general, the external resistance is negligible when Bi is greater than 10,(Carta and Jungbauer, 2010). According to LeVan and Carta (2007), the Sherwood number is always larger than 2 and typically larger than 10 in packed columns. Since D_e/D_o is less than 1 when pore diffusion is dominant, Bi >> 1, making the external resistance negligible. Different results may be obtained when surface diffusion is dominant. In this case intraparticle transport can be much faster than boundary layer mass transfer, making the latter the dominant resistance.

3. Experimental

3.1 Materials

3.1.1 Stationary phases

The cation exchangers used in this study are UNOsphere Rapid S and Nuvia S from Bio-Rad Laboratories (Hercules, CA, USA), and POROS 50HS from Applied Biosystems (Foster City, CA, USA). UNOsphere Rapid S and Nuvia S are based on a similar macroporous polymeric backbone, but Nuvia S contains grafted charged polymeric surface extenders. POROS 50HS is based on a cross linked poly(styrene-divinylbenzene) matrix. All three resins contain sulfopropyl functional groups. Mean particle sizes are 100, 85, 50 µm for UNOsphere Rapid S, Nuvia S, and POROS 50HS, respectively.

3.1.2 Proteins and buffers

Three purified mAbs identified as mAb A, mAb B, and mAb C (M_r~150kDa) were obtained from MedImmune (Gaithersburg, MD, USA). Other proteins used in this study were obtained from Sigma-Aldrich (St. Louis, MO, USA) and included, thyroglobulin (M_r-660kDa), bovine serum albumin (BSA) (M_r~67kDa), and lactalbumin (M_r~14kDa). All proteins were used as received without further purification.

Acetate buffers were prepared with fixed concentrations of sodium and arginine for use at pH 5.0 using sodium acetate, free-base arginine, and acetic acid. For use at pH 6.0, 2-(N-morpholino)ethanesulfonic acid (MES) buffers were prepared using sodium hydroxide, free base arginine and monohydrate MES. For use at pH 7 and 7.5, phosphate buffers were prepared using dibasic sodium phosphate (Na_2HPO_4), free-base arginine, and phosphoric acid. Buffer solutions containing sodium chloride were prepared by first adding sodium chloride and then titrating with the correct acid to the desired pH. All chemicals used in this study were analytical reagent grade

and were obtained from Fisher Scientific (Pittsburgh, PA, USA) and Sigma Aldrich (St. Louis, MO, USA).

3.2 Methods:

3.2.1 Iso-Electric Focusing

Iso-electric focusing experiments were performed to determine the iso-electric points (pI) of the three mAbs, and were performed on a Multiphor II unit (GE Healthcare, Piscataway, NJ, USA) according to the equipment manufacturer's instructions. An iso-gel agarose plate with a pH gradient of 3 to 10 (Lonza, Rockland, ME, USA) was placed in the center of the apparatus. Anode and cathode wicks were then placed on the negative and positive electrode contacts of the apparatus. A sample applicator mask was placed across the gel 3 cm away from the cathode wick. 10 μg samples of mAb and standards (Bio-Rad, Hercules, CA, USA) were then placed into the slots of the mask. The power limit was then set to 1 W for 10 minutes to pre-focus the samples. The mask was then removed and the power and voltage were set to 25 W and 1,500 volts respectively for 75 minutes. The gel was then fixed using a solution containing 36% (v/v) methanol, 3.6% (w/v) sulphosalicylic acid and 6% (w/v) tricholoacetic acid and then washed using deionized water. Following the wash, the gel was stained with Coomassie Blue stain, washed with deionized water again, and rinsed with a Coomassie destaining solution to remove any excess stain.

3.2.2 Analysis under non-binding conditions

The Height Equivalent to a Theoretical Plate (HETP) was measured for UNOsphere Rapid S, Nuvia S, and POROS 50HS to determine their mass transfer properties.. For this purpose, each resin was flow-packed into Tricorn 0.5x5 cm columns using a 20 mM sodium acetate buffer with 1 M NaCl with an AKTA Explorer 10 unit (GE Healthcare) using Unicorn

operating software. The packing velocity for each resin was selected according to each resin's manufacture recommendations. The experiments were performed under non-binding conditions (1 M NaCl) to avoid the potential influence of electrostatic interactions on transport. The HETP was obtained by the moment method (Carta and Jungbauer, 2010). and the effective pore diffusivity, D_e , was calculated from the slope of plots of reduced HETP, h (=HETP/d_p) vs. reduced velocity, v'=(vd_p/D_o) using the following equation (Carta, et al., 2005):

$$\frac{D_e}{D_0} = \frac{1}{30}\frac{\varepsilon}{1-\varepsilon}\left(\frac{k'}{1+k'}\right)^2\frac{1}{c}$$

(3.1)

where d_p is the particle diameter, v the mobile phase interstitial velocity, the extraparticle porosity, D_o the protein free solution diffusivity, k' the retention factor and c the slope of h vs. v'.

3.2.3 Linear gradient elution

Linear gradient elution (LGE) experiments were conducted on UNOsphere Rapid S, Nuvia S, and POROS 50HS to determine the retention of the three mAbs and aggregates according to the procedure of Yamamoto (1995). The columns used were the same as the columns used to determine HETPs. Each column was initially equilibrated with a buffer solution containing 20 mM of sodium or arginine, loaded with 0.1 mL samples containing 2 mg/mL of mAb prepared in an acetate buffer at pH 5, and eluted from the column by increasing the counterion concentration in a linear gradient at the column entrance. The mobile phase flow rate was varied from 0.25 mL/min to 2 mL/min.

3.2.4 Low pH mAb aggregation

Soluble aggregates were produced by slowly acidifying 1.5 mL of a mAb at a concentration of approximately 10 mg/mL in initially present 8 mM histidine and 50mM NaCl at

pH 6. The solution was stirred continuously while 0.1 M HCl was added drop-wise until the solution reached pH 2.8. The mixture was then stirred at room temperature (22 ˚C) for 48 hrs. The solution was then quenched to pH 5 by adding 50 mM sodium acetate at pH 5.

3.2.5 Size exclusion chromatography

Size exclusion chromatography (SEC) experiments were performed using a Superdex 200, 10/300GL column from GE Healthcare. 30 µL of 2 g/L samples of thyroglobulin, BSA, lactalbumin, mAb and mAb soluble aggregates were injected at a flow rate of 0.5 mL/min with a Waters Mod. 2595 HPLC unit. Detection was with a Thermo Fischer Scientific UV1000 detector (San Jose, CA, USA).

3.2.6 Dynamic light scattering

3.2.6.1 Batch dynamic light scattering

Batch mode dynamic light scattering experiments were performed at 25 ˚C with a DynaPro Nanostar Instrument from Wyatt Technology Corporation (Santa Barbara, CA, USA). Approximately 0.1 mL of mAb or mAb aggregate at a concentration of approximately 2 mg/mL was filtered though a 0.22 µm syringe filter into a disposable cuvette. The curvette was then placed in the NanoStar instrument and measurements were made using Dynamics Software from Wyatt Technology Corporation to determine the hydrodynamic radius of the molecules in solution.

3.2.6.2 In-line dynamic light scattering

In-line dynamic light scattering experiments were performed at 25 ˚C using a DynaPro Nanostar Instrument from Wyatt Technology Corporation (Santa Barbara, CA, USA) interfaced to a MiniDawn Treos unit also from Wyatt Technology Corporation with a fiber optic. 100 µL of

a mAb aggregate solution was injected into a POROS 50HS or Superdex 200 10/300GL column using at a flow rate of 0.5 mL/min with a Waters Mod. 2595 HPLC unit. The solution was then flowed through the Mini Dawn Treos instrument.

4. Results and Discussion

4.1 Characterization of individual mAbs

Figure 4.1 shows the isoelectric focusing (IEF) results of the three mAbs and standards. The results show that mAb A contained 3 major charge variants, mAb B contained 2 major charge variants and mAb C contained only a single major variant. However, all mAb variants fell within a narrow pI range, as summarized in Table 4.1.

4.2 Single Component Linear Gradient Elution

4.2.1 Effect of mAb Type

Linear gradient elution experiments were conducted to determine the retention characteristics of the individual mAbs according to the method of Yamamoto (1995). Following Carta and Jungbauer (2010), at low protein loads the relationship between the normalized gradient slope, $\gamma = \beta L / \nu$, and the counterion concentration at which the protein elutes, C_B^R, in linear gradient elution is given by the following equation:

$$\gamma = \int_{C_B^o}^{C_B^R} \frac{dC_B}{k' - k'_M} \tag{4.1}$$

where $k' = k'_M + \phi m$ is the protein retention factor at C_B, C_B^o the initial counterion concentration, m the linear binding isotherm slope, and k'_M the protein retention factor under non-binding conditions. Based on the non-binding experiments described in Section 4.3.1, the k'_M values were 0.4, 1.0, 1.2 for Nuvia S, POROS 50HS, and UNOSphere Rapid S, respectively. Combining eq. 2.6 on page 7 and eq. 4.1, for a
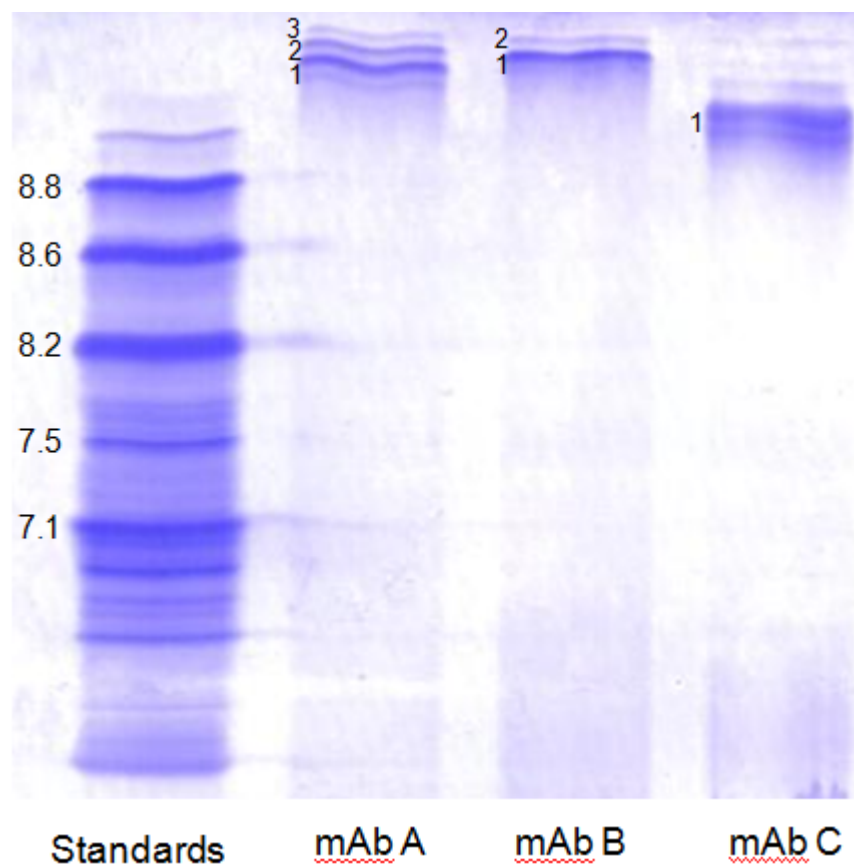
Figure 4.1. IEF of mAbs A,B, and C and standards.

Band	mAb A	mAb B	mAb C
1	9.1	9.1	9.0
2	9.1	9.1	-
3	9.2	-	-

Table 4.1. Iso-electric points of each charge variant band

monovalent counterion with z_B equal to one, such as Na^+ used in this work, and then integrating yields:

$$\gamma = \frac{\left(C_B^R\right)^{z_P+1} - \left(C_B^o\right)^{z_P+1}}{A(z_P+1)} \tag{4.2}$$

where $A = \phi K_{P,B} q_o^{z_P}$. In practice, z_P is usually large and C_B^R is often small. Thus only the first term in the numerator is important. Under those conditions, eq. 4.2 simplifies to $\gamma \sim \left(C_B^R\right)^{z_P+1}/A(z_P+1)$, or $\log \gamma = (z_P+1)\log C_B^R - \log A(z_P+1)$ giving a linear plot of log γ vs. log C_B^R with a slope equal to z_p+1, and an intercept equal to $-\log A(z_P+1)$.

Figures 4.2a, b, and c show typical chromatograms for mAb A, B and C at pH 5 on Nuvia, UNOsphere, and POROS, respectively, with different gradient slopes. From the plots, one can see that mAb A and C consistently elute at a very similar sodium concentrations on each resin for a given gradient slope, whereas mAb B elutes at slightly lower concentrations.

Figure 4.3 shows log-log plots of γ vs. C_B^R for the chromatograms shown in Fig. 4.2. From these plots, we can see that POROS exhibits the highest binding strength for each mAb, UNOsphere has an intermediate binding strength close to that of POROS, whereas Nuvia consistently displays the lowest binding strength for each mAb..

The regressed values of z_p and A are shown in Table 4.2. The values of z_p and A varied for each mAb suggesting that differences exist in the way each mAb interacts with the three different resins.

Figure 4.2a. Linear gradient elution (LGE) chromatograms obtained for Nuvia S for mAb A, mAb B, and mAb C at different gradient slopes and (d) overlaid chromatograms of mAb A, B, and C with a 15 gradient slope. The mobile phase was 20 mM sodium acetate at pH 5 with a final sodium chloride concentration of 500 mM. The gradient durations were 15, 20, 25, and 30 column volumes.
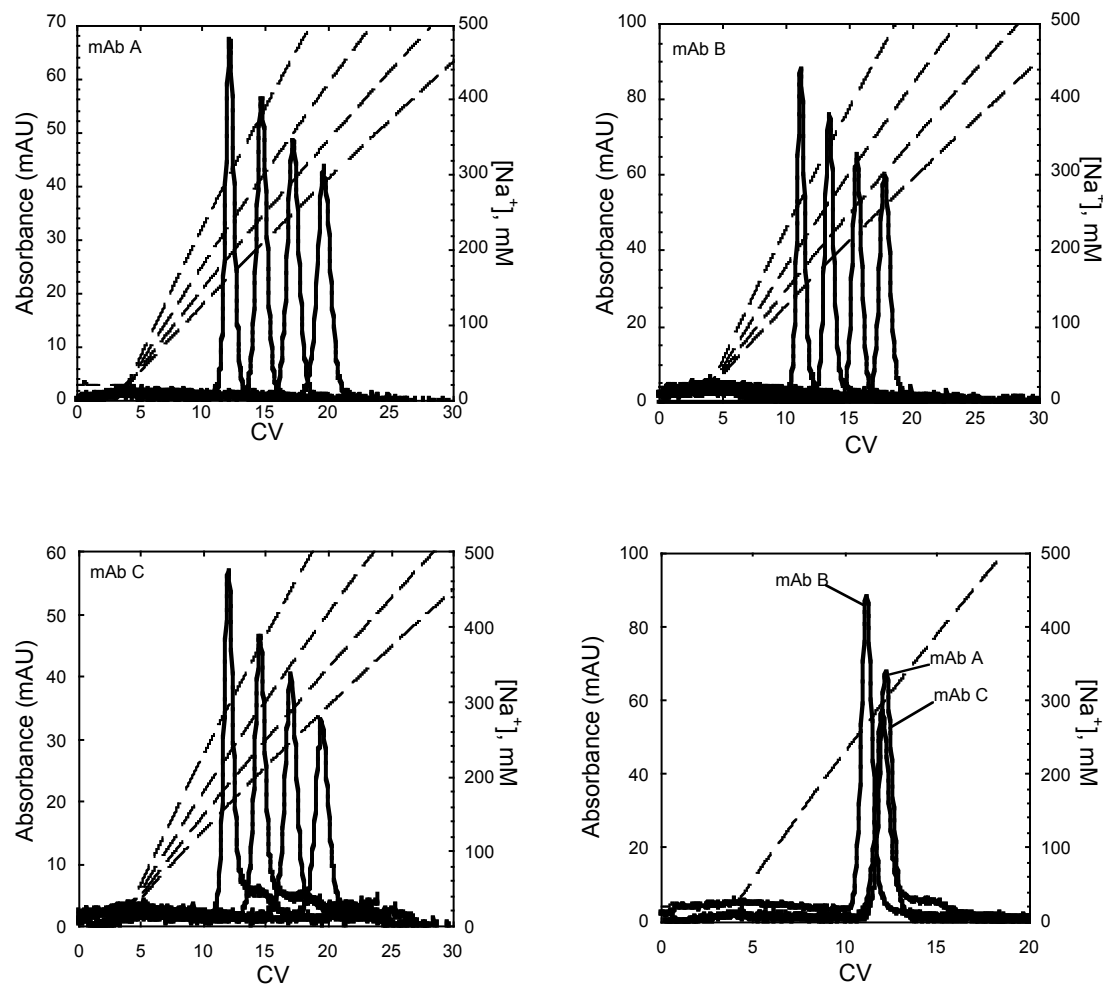
Figure 4.2b. Linear gradient elution (LGE) chromatograms obtained for POROS 50HS for mAb

A, mAb B, and mAb C at different gradient slopes and (d) overlaid chromatograms of mAb A,

B, and C with a 15 gradient slope. The mobile phase was 20 mM sodium acetate at pH 5 with a

final sodium chloride concentration of 500 mM. The gradient durations were 15, 20, 25, and 30

column volumes.

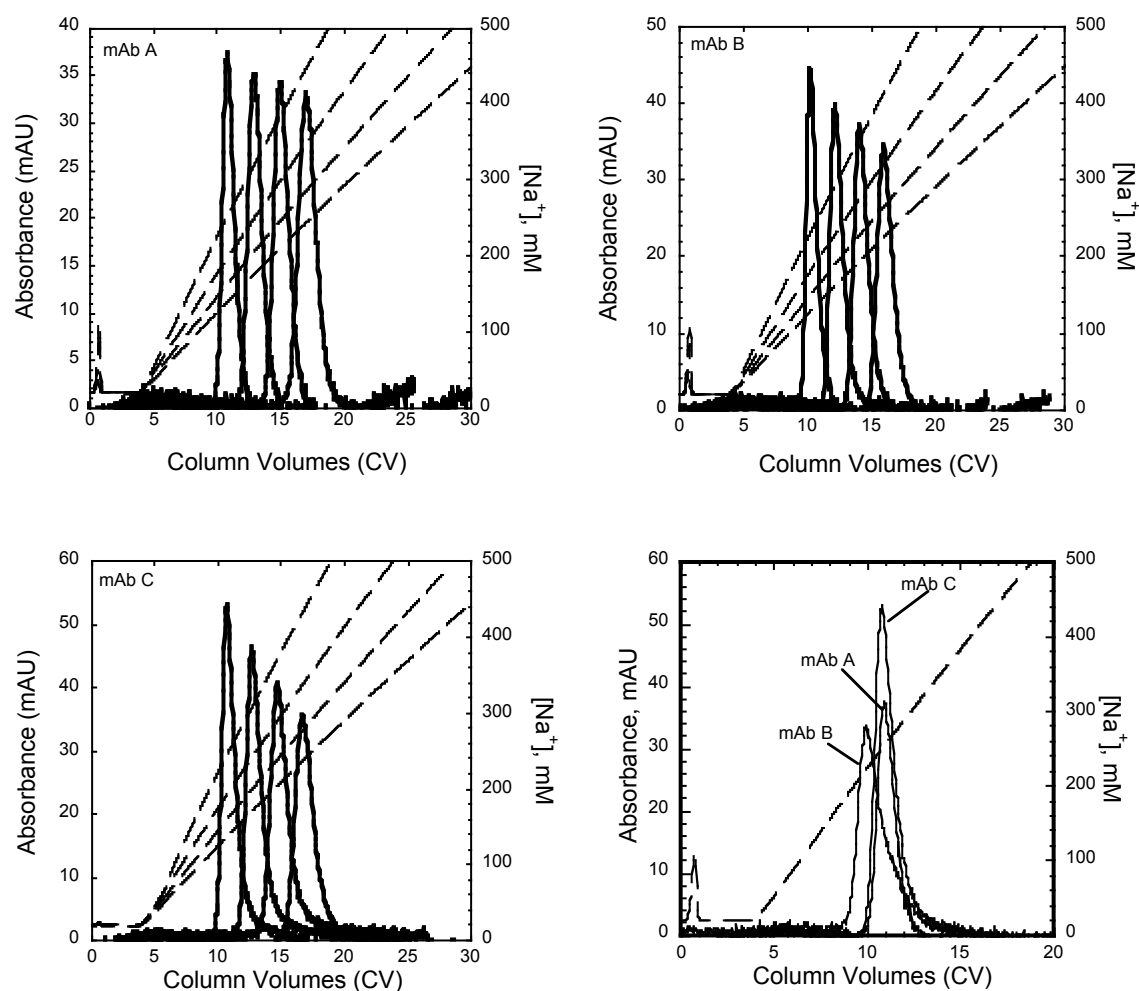Figure 4.2c. Linear gradient elution (LGE) chromatograms obtained for UNOsphere Rapid S for mAb A, mAb B, and mAb C at different gradient slopes and (d) overlaid chromatograms of mAb A, B, and C with a 15 gradient slope. The mobile phase was 20 mM sodium acetate at pH 5 with a final sodium chloride concentration of 500 mM. The gradient durations 15, 20, 25, and 30 column volumes.
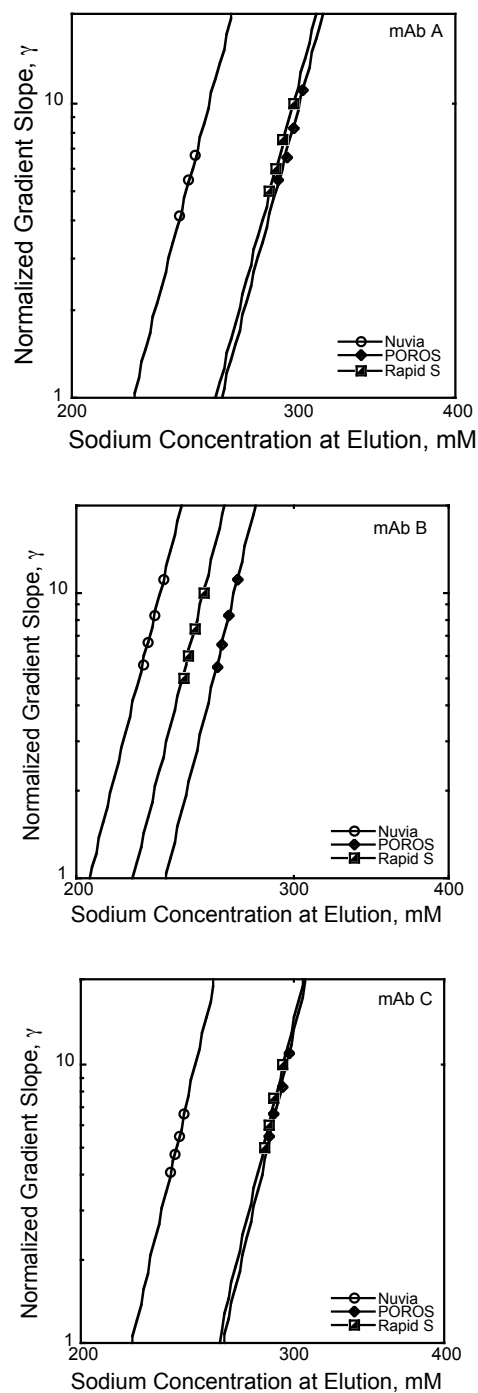
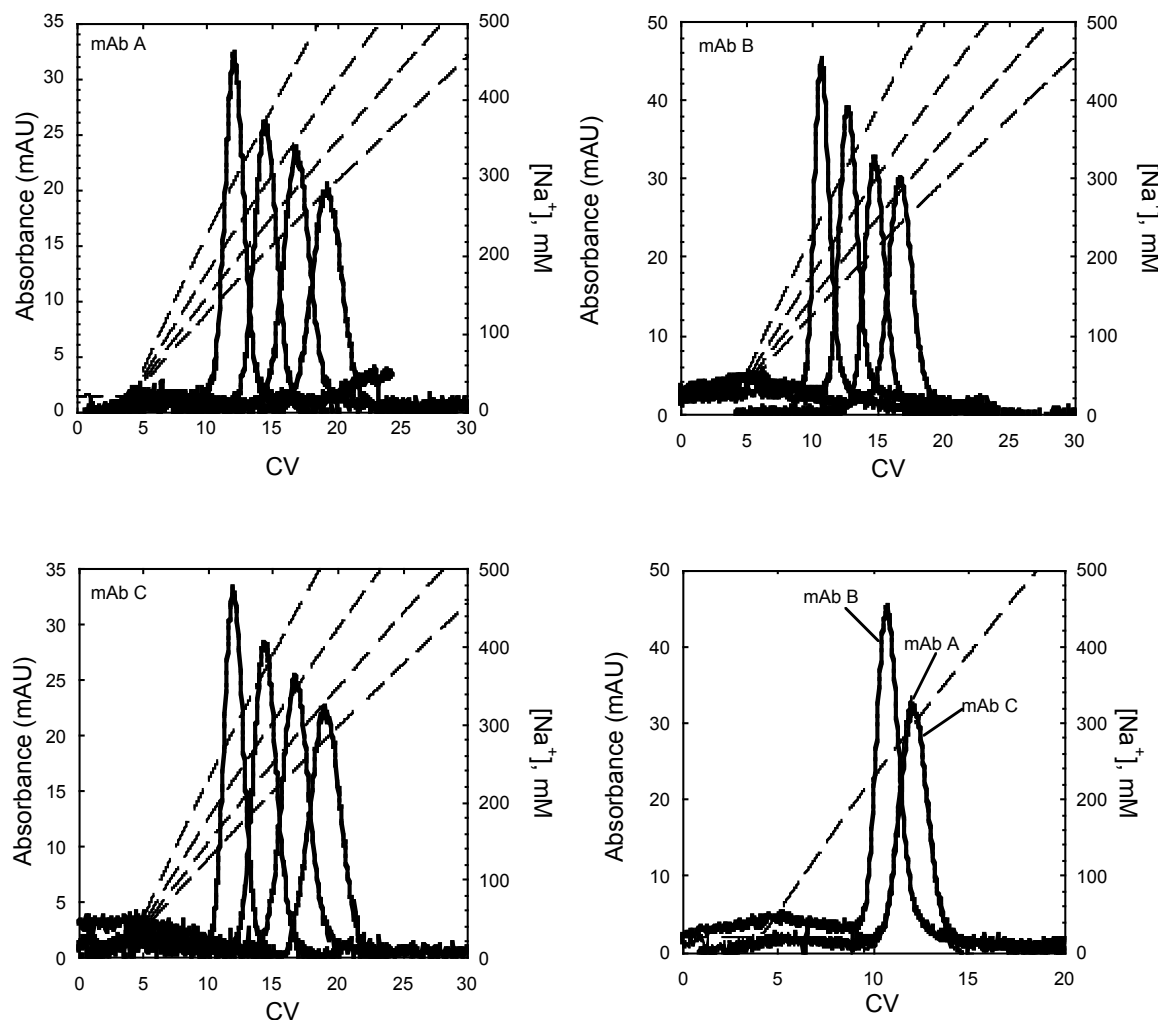Figure 4.3. Plots of normalized gradient slope vs. sodium concentration at elution on logarithmic axes for mAb A, mAb B, and mAb C. Mobile phase conditions were 20 mM sodium acetate at pH 5 with a final sodium chloride concentration of 500 mM.

Table 4.2. Retention parameters for mAb A, B, and C at pH 5 for Nuvia S, POROS 50HS, and UNOsphere Rapid S

Resin Type	mAb	Effective Charge, z_P	Affinity Coefficient, A
Nuvia S	A	15.1±0.7	2.28×10^{35}
	B	16.6±0.5	2.45×10^{39}
	C	17.8±1.0	4.72×10^{42}
POROS 50HS	A	15.2±0.9	8.89×10^{37}
	B	17.0±0.8	3.57×10^{41}
	C	17.9±0.7	2.56×10^{44}
UNOsphere Rapid S	A	15.8±0.2	1.84×10^{39}
	B	16.5±0.7	5.77×10^{39}
	C	17.4±0.6	1.17×10^{43}

There was no statistically significant difference in the effective charge of each mAb on a given resin; however, the affinity coefficient, A, varied substantially from resin to resin. This difference can attributed to different factors including hydrophobic interactions between the mAb and resin backbone or different functional group linkers which could affect the way the protein and functional group interact.

Based on the regressed values of z_p and A, protein retention factors, $k'-k_M$, were determined for each mAb. Figure 4.4 shows $k'-k_M$, plotted against the sodium concentration for mAb A, B and C at pH 5 on Nuvia, UNOsphere, and POROS. These plots show that mAb A and C have almost identical retention factors on UNOsphere whereas mAb C has lower retention. On the other hand, the retention of each mAb is slightly different for both Nuvia and POROS but we can see that the difference between all three is much smaller than that for UNOsphere.

4.2.2 Effect of pH

Linear gradient elution experiments were performed to determine the effect of pH on retention. Figures 4.5a-f show chromatograms obtained for mAb A, B, and C on Nuvia, UNOsphere and POROS at pH values of 6 and 7. From these graphs, it can be seen that increasing pH affects each mAb differently. At pH 5, mAb A and C eluted at almost identical sodium concentrations. The trend changed as the pH increased to 7, where B and C eluted at similar concentrations and mAb A eluted at a higher concentration.

It is also apparent that the resin type has a more pronounced effect as the pH increases. For UNOsphere, as the buffer pH increased the mAbs eluted at increasingly different sodium concentrations. The UNOsphere results are different than Nuvia, which
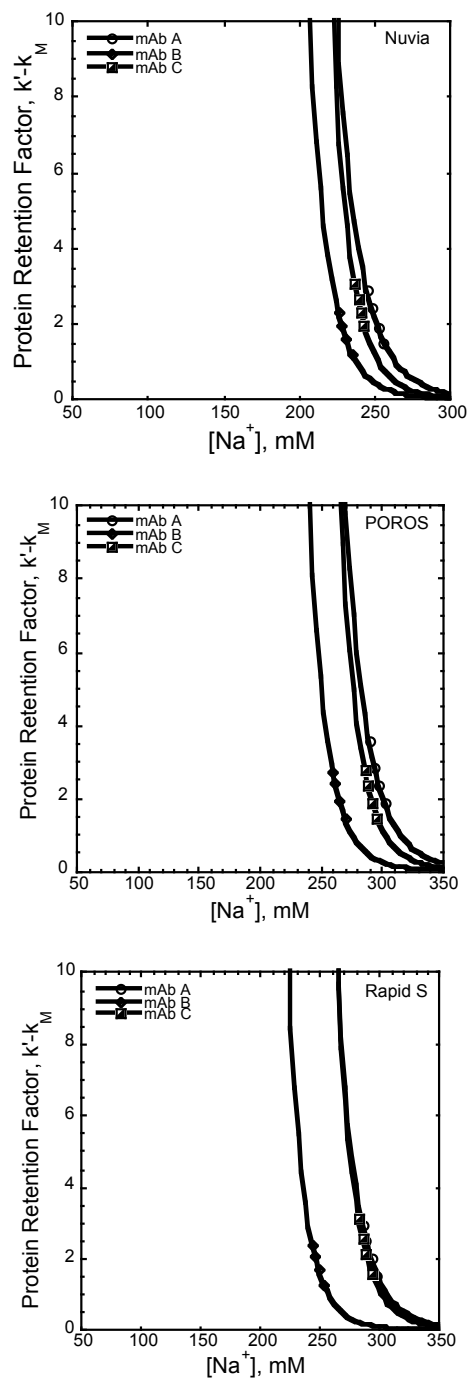
Figure 4.4. Retention factor of mAb A, B, and C at pH 5 for Nuvia S, POROS 50HS, and UNOsphere Rapid S
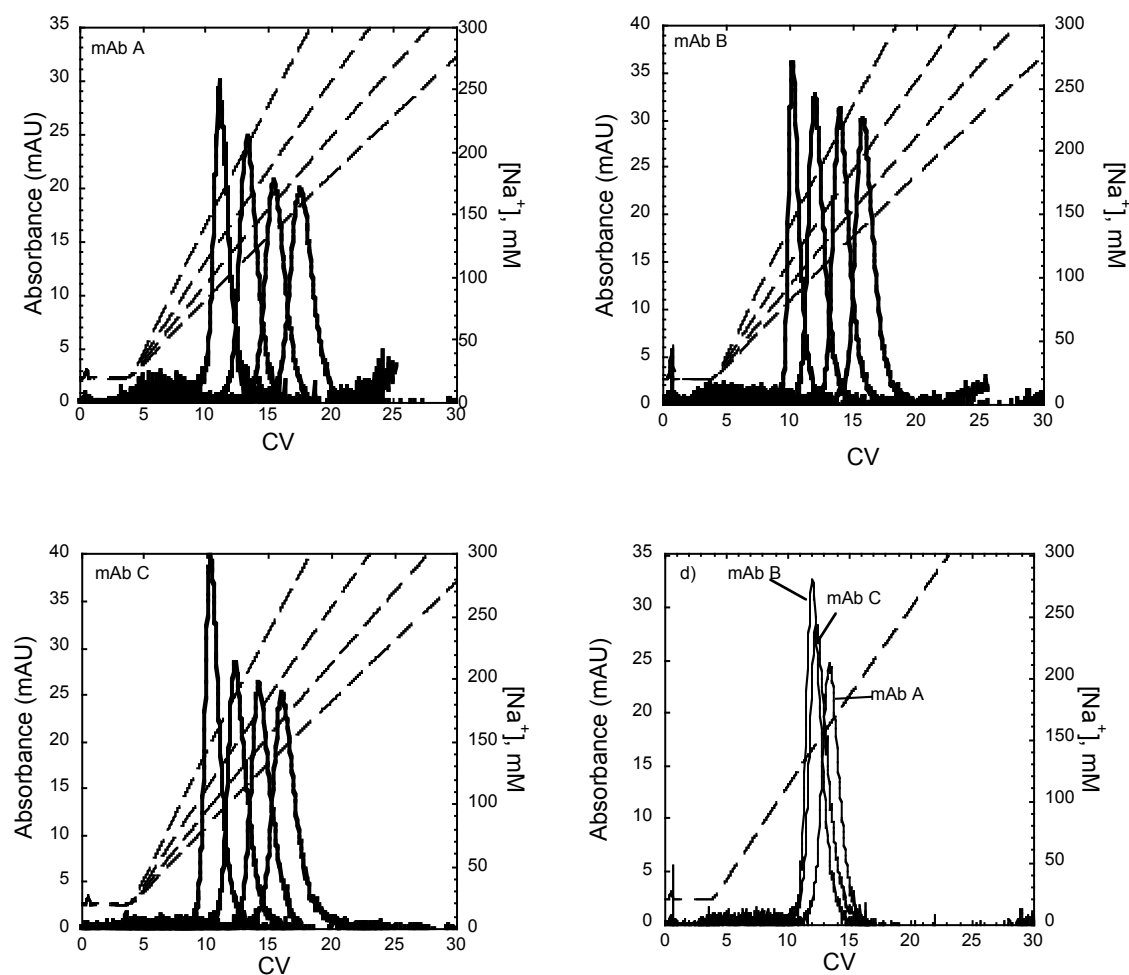
Figure

4.5a. Linear gradient elution (LGE) chromatograms obtained for Nuvia S for mAb A, mAb B, and mAb C at different gradient slopes and (d) overlaid chromatograms of mAb A, B, and C with a 20 gradient slope. The mobile phase was 20 mM sodium MES at pH 6 with a final sodium chloride concentration of 320 mM. The gradient durations were 15, 20, 25, and 30 column volumes.

Figure 4.5b. Linear gradient elution (LGE) chromatograms obtained for Nuvia S for mAb A, mAb B, and mAb C at different gradient slopes and (d) overlaid chromatograms of mAb A, B, and C with a 20 gradient slope. The mobile phase was 20 mM sodium phosphate at pH 7 with a final sodium chloride concentration of 220 mM. The gradient durations were 15, 20, 25, and 30 column volumes.
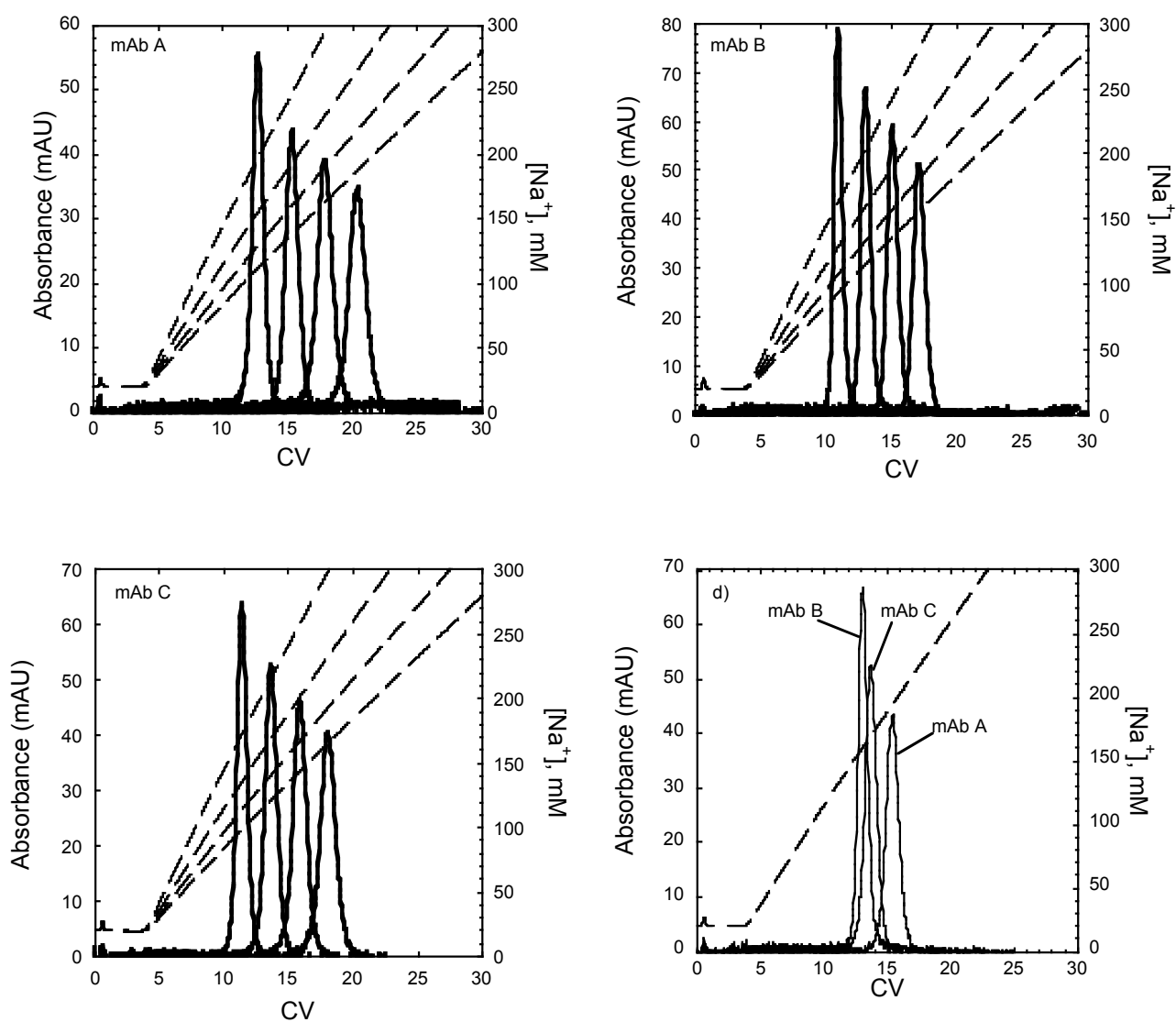
Figure 4.5c. Linear gradient elution (LGE) chromatograms obtained for POROS 50HS for mAb A, mAb B, and mAb C at different gradient slopes and (d) overlaid chromatograms of mAb A, B, and C with a 20 gradient slope. The mobile phase was 20 mM sodium MES at pH 6 with a final sodium chloride concentration of 320 mM. The gradient durations were 15, 20, 25, and 30 column volumes.
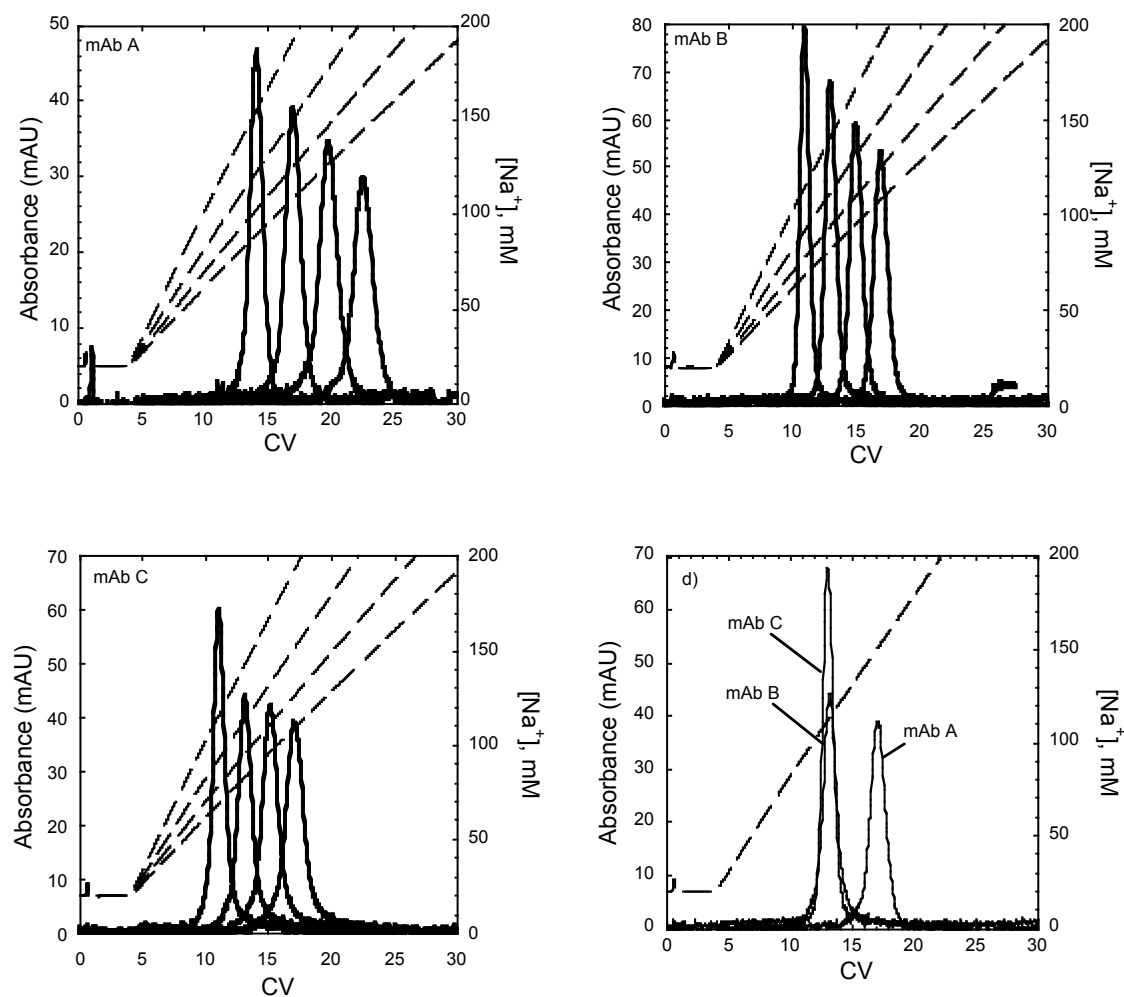
Figure 4.5d. Linear gradient elution (LGE) chromatograms obtained for POROS 50HS for mAb A, mAb B, and mAb C at different gradient slopes and (d) overlaid chromatograms of mAb A, B, and C with a 20 gradient slope. The mobile phase was 20 mM sodium phosphate at pH 7 with a final sodium chloride concentration of 220 mM. The gradient durations were 15, 20, 25, and 30 column volumes.
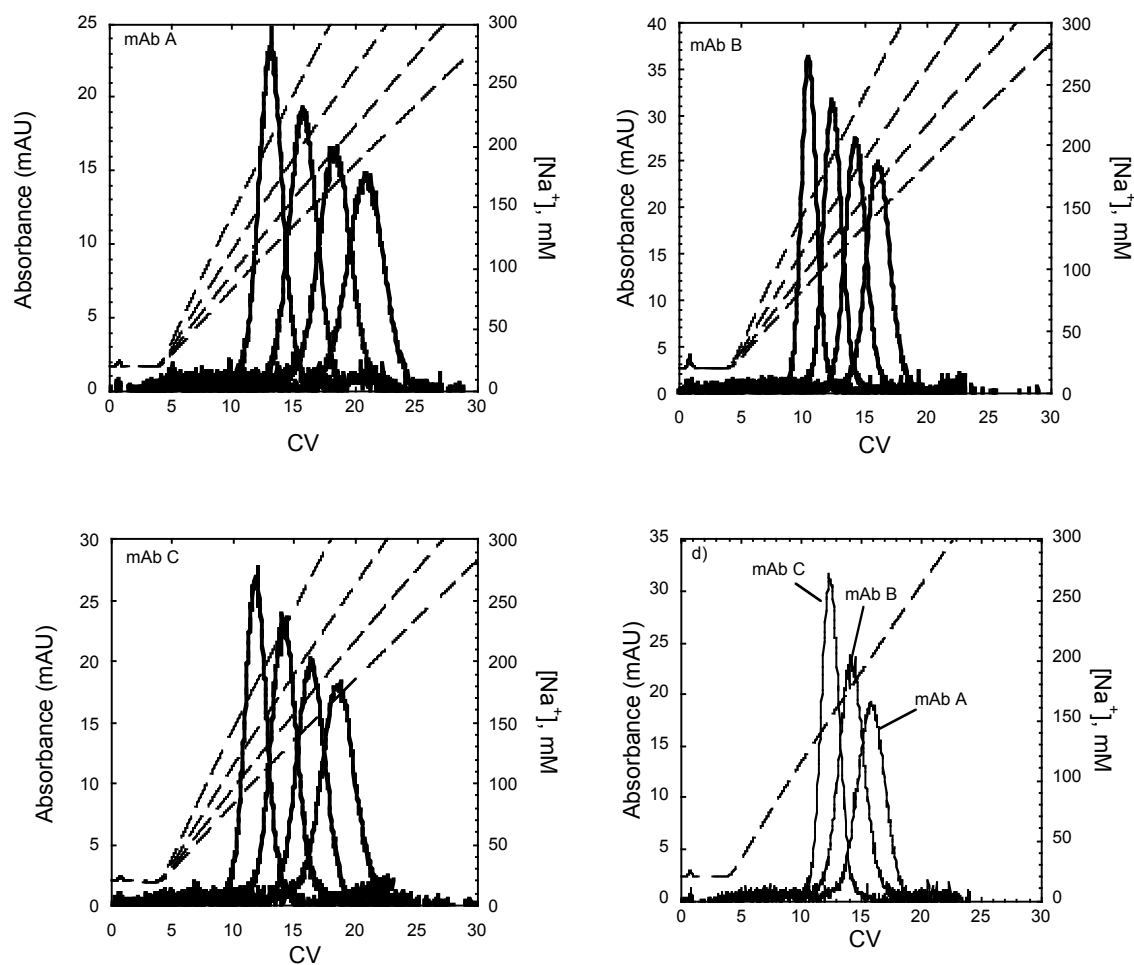
Figure 4.5e. Linear gradient elution (LGE) chromatograms obtained for UNOsphere Rapid S for mAb A, mAb B, and mAb C at different gradient slopes and (d) overlaid chromatograms of mAb A, B, and C with a 20 gradient slope. The mobile phase was 20 mM sodium MES at pH 6 with a final sodium chloride concentration of 320 mM. The gradient durations were 15, 20, 25, and 30 column volumes.
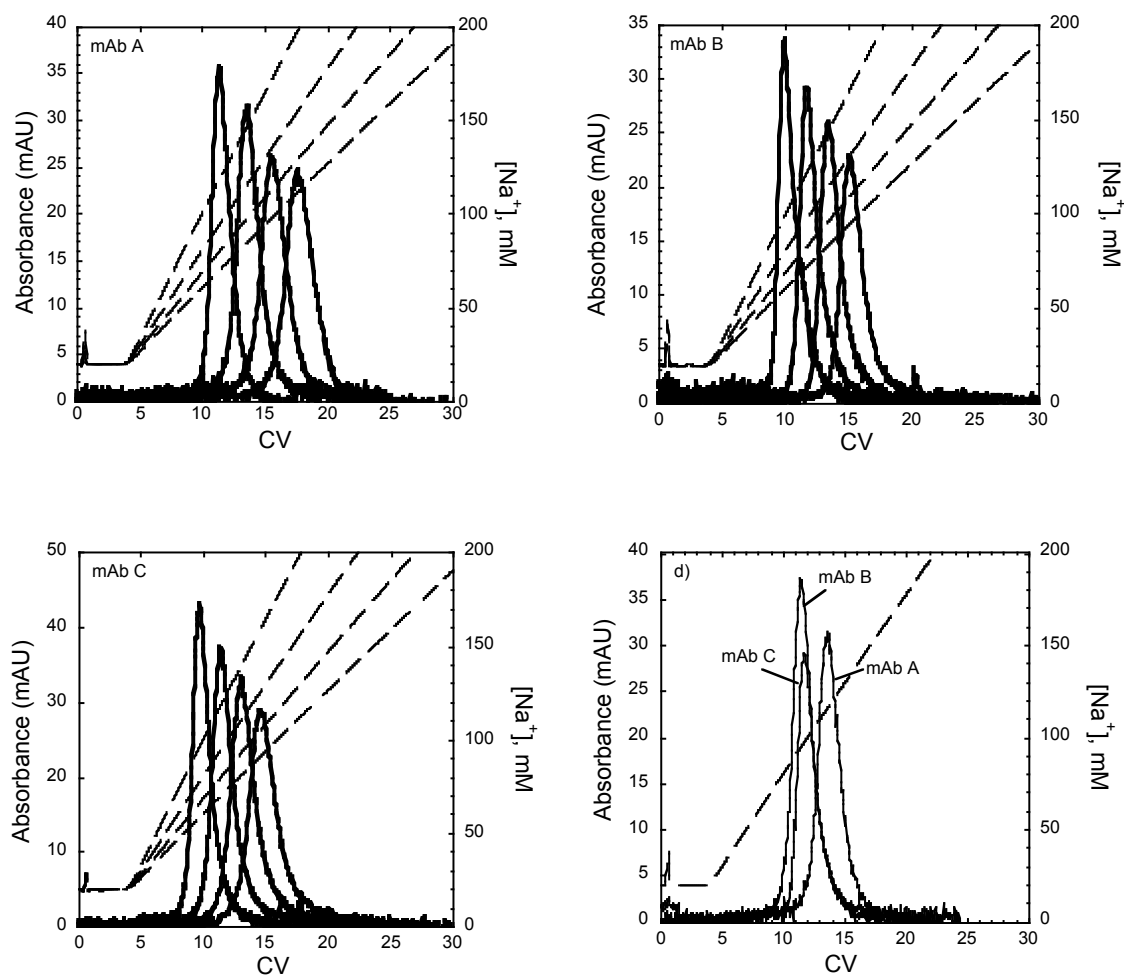
Figure 4.5f. Linear gradient elution (LGE) chromatograms obtained for UNOsphere Rapid S for mAb A, mAb B, and mAb C at different gradient slopes and (d) overlaid chromatograms of mAb A, B, and C with a 20 gradient slope. The mobile phase was 20 mM sodium phosphate at pH 7 with a final sodium chloride concentration of 220 mM. The gradient durations were 15, 20, 25, and 30 column volumes.
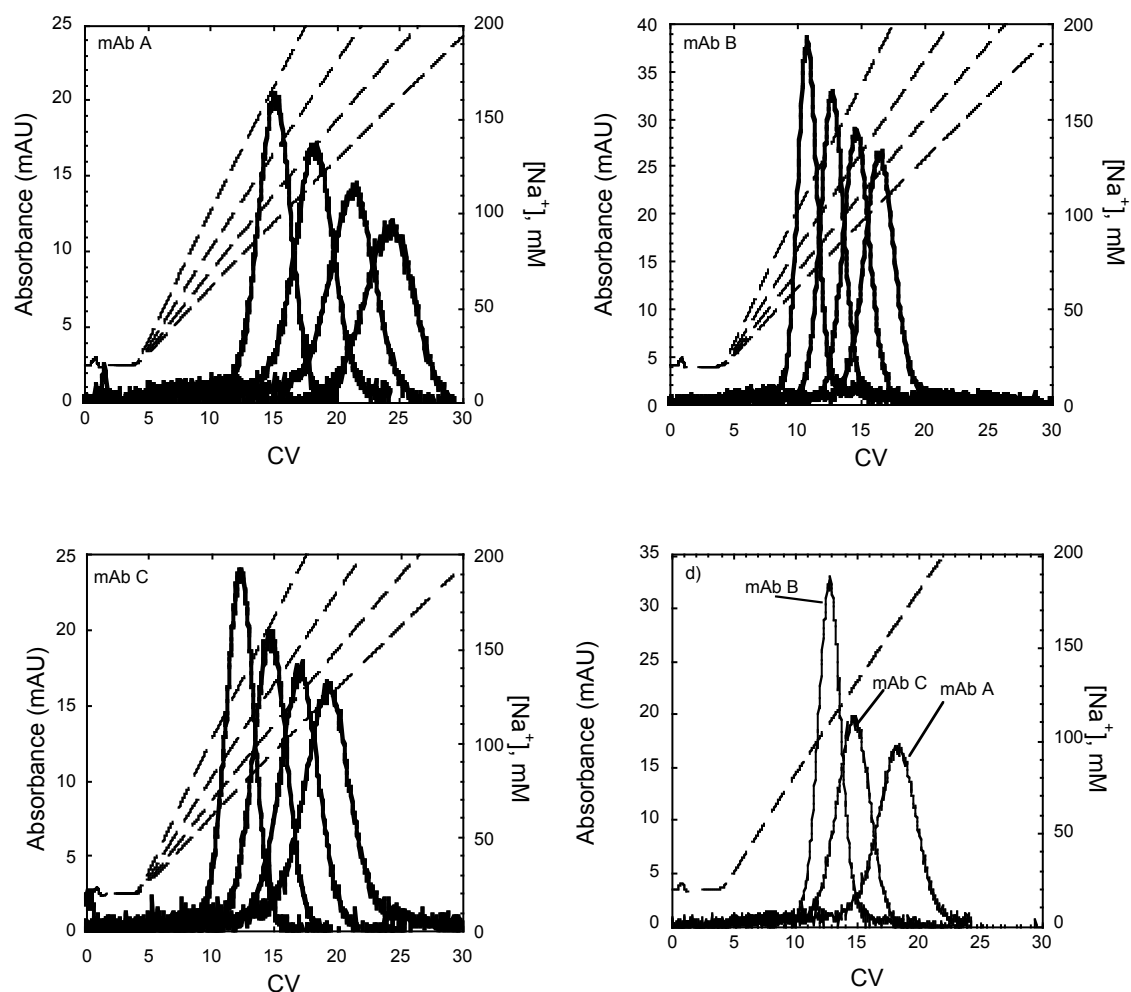
had all three mAbs elute at very similar sodium concentrations at pH 6 and 7. The elution peaks on POROS followed the same trend as Nuvia but at pH 7 mAb A eluted at a much higher concentration than B and C.

The regressed values z_P and A at pH 5, 6 and 7 are shown in Table 4.3. As expected, the values for z_P and A decreased as the pH of the buffer approached the pI of the mAbs and their net charge decreased. Figures 4.6a, b and c show the corresponding calculated retention factors mAbs A, B and C on Nuvia, UNOsphere, and POROS at all three pH values. For all three resins, increasing pH shifted the k' values of mAb B and C closer together. For both Nuvia and POROS, pH 7 gave no discernable difference between mAb B and mAb C although significant differences existed for UNOsphere.

4.2.3 Effect of counterion type

Linear gradient elution experiments were conducted with arginine as the counterion instead of sodium for otherwise identical conditions. Figures 4.7a-i show chromatograms for Nuvia, POROS, and UNOsphere, respectfully. As in the case of sodium, the chromatograms show that at pH 5 mAb A and C consistently elute at very similar arginine concentrations for each resin, whereas mAb B elutes at slightly lower concentrations. At pH 7, mAb B and C elute at approximately the same counterion concentration. Table 4.4 contains the regressed values of z_p and A with arginine as the counterion. The values for z_p obtained were consistent with those obtained with sodium This result suggests that the stoichiometry of the protein ion exchange process is the same regardless of the counterion used. The affinity parameter varied only slightly.

Table 4.3. Retention parameters for mAb A, B, and C at pH 5, 6 and 7 for Nuvia S, POROS 50HS, and UNOsphere Rapid S.

Resin	pH	mAb	Effective Charge, z_P	Affinity Parameter, A
Nuvia S	5	A	15.1±0.7	2.28×10^{35}
		B	16.6±0.5	2.45×10^{39}
		C	17.8±1.0	4.72×10^{42}
	6	A	11.6±0.5	1.41×10^{26}
		B	12.7±0.3	3.84×10^{27}
		C	13.7±0.9	9.10×10^{29}
	7	A	9.3±0.3	5.76×10^{19}
		B	11.3±0.5	7.91×10^{22}
		C	10.7±0.4	3.39×10^{21}
UNOsphere Rapid S	5	A	15.8±0.2	1.84×10^{39}
		B	16.5±0.7	5.77×10^{39}
		C	17.4±0.6	1.17×10^{43}
	6	A	11.6±0.5	1.70×10^{27}
		B	12.9±0.9	2.98×10^{28}
		C	13.3±0.3	1.92×10^{30}
	7	A	9.4±0.3	3.21×10^{21}
		B	11.4±0.6	5.02×10^{23}
		C	10.5±0.4	5.06×10^{22}
POROS 50HS	5	A	15.2±0.9	8.89×10^{37}
		B	17.0±0.8	3.57×10^{41}
		C	17.9±0.7	2.56×10^{44}
	6	A	11.6±0.5	1.51×10^{27}
		B	12.6±0.5	1.94×10^{28}
		C	13.6±0.2	6.52×10^{30}
	7	A	9.3±0.3	6.32×10^{20}
		B	11.3±0.7	4.34×10^{23}
		C	10.8±0.5	5.54×10^{22}

Figure 4.6a. Retention factors of mAb A, B, and C at (A) pH 5, (B) pH 6, and (C) pH 7 on Nuvia S.
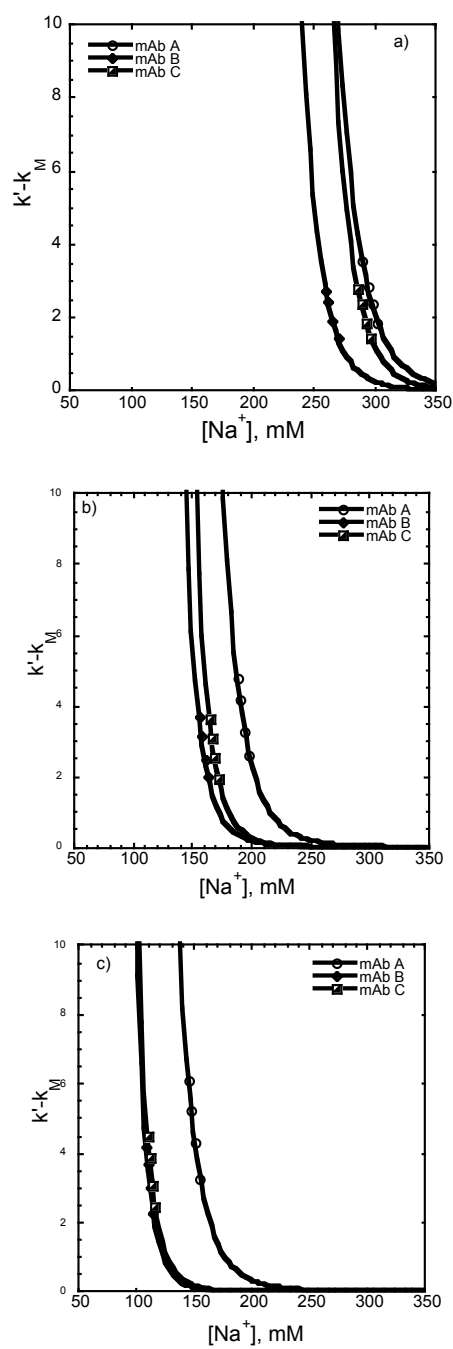
Figure 4.6b. Retention factors of mAb A, B, and C at (A) pH 5, (B) pH 6, and (C) pH 7 on POROS 50HS.
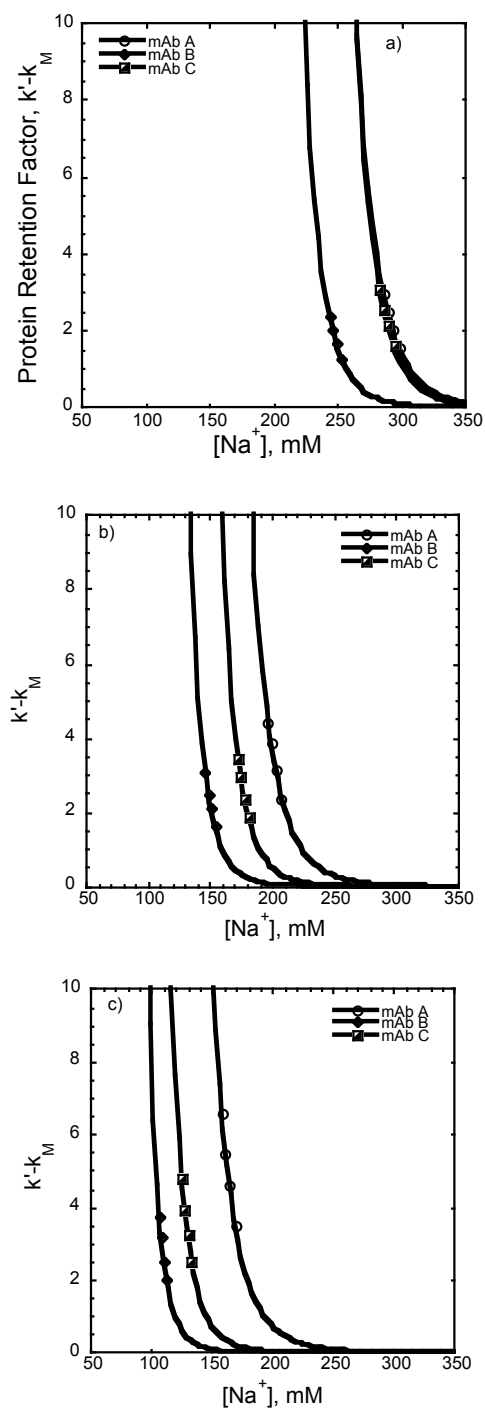
Figure 4.6c. Retention factors of mAb A, B, and C at (A) pH 5, (B) pH 6, and (C) pH 7 on UNOsphere Rapid S.

Figure 4.7a. Linear gradient elution (LGE) chromatograms obtained for Nuvia S for mAb A, mAb B, and mAb C at different gradient slopes. The mobile phase was 20 mM arginine acetate at pH 5 with a final arginine concentration of 488 mM. The gradient durations were 15, 20, 25, and 30 column volumes.

Figure 4.7b. Linear gradient elution (LGE) chromatograms obtained for Nuvia S for mAb A, mAb B, and mAb C at different gradient slopes. The mobile phase was 20 mM arginine MES at pH 6 with a final arginine concentration of 300 mM. The gradient durations were 15, 20, 25, and 30 column volumes.
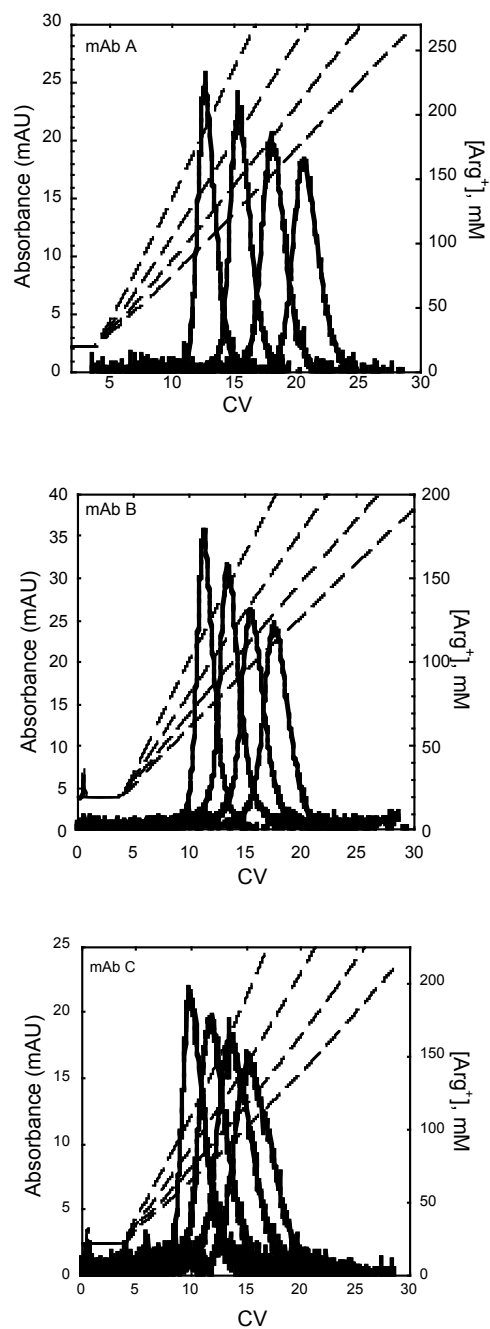
Figure 4.7c. Linear gradient elution (LGE) chromatograms obtained for Nuvia S for mAb A, mAb B, and mAb C at different gradient slopes. The mobile phase was 20 mM arginine phosphate at pH 7 with a final arginine concentration of 250 mM. The gradient durations in were 15, 20, 25, and 30 column volumes.
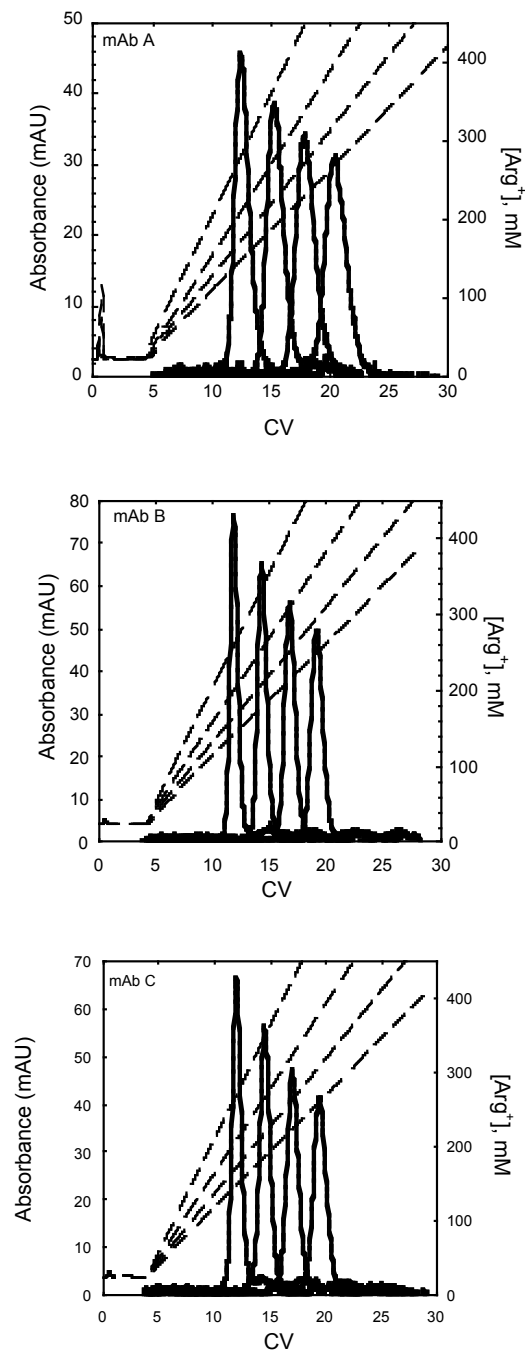
Figure 4.7d. Linear gradient elution (LGE) chromatograms obtained for POROS 50HS for mAb A, mAb B, and mAb C at different gradient slopes. The mobile phase was 20 mM arginine acetate at pH 5 with a final arginine concentration of 488 mM. The gradient durations in were 15, 20, 25, and 30 column volumes.
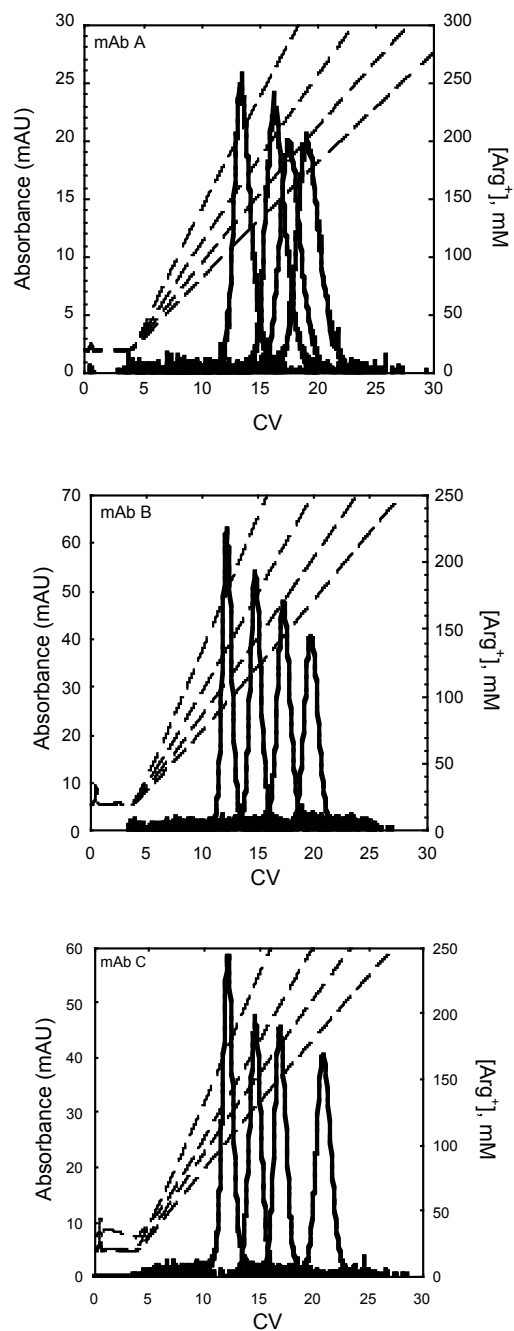
Figure 4.7e. Linear gradient elution (LGE) chromatograms obtained for POROS 50HS for mAb A, mAb B, and mAb C at different gradient slopes. The mobile phase was 20 mM arginine MES at pH 6 with a final arginine concentration of 300 mM. The gradient durations were 15, 20, 25, and 30 column volumes.
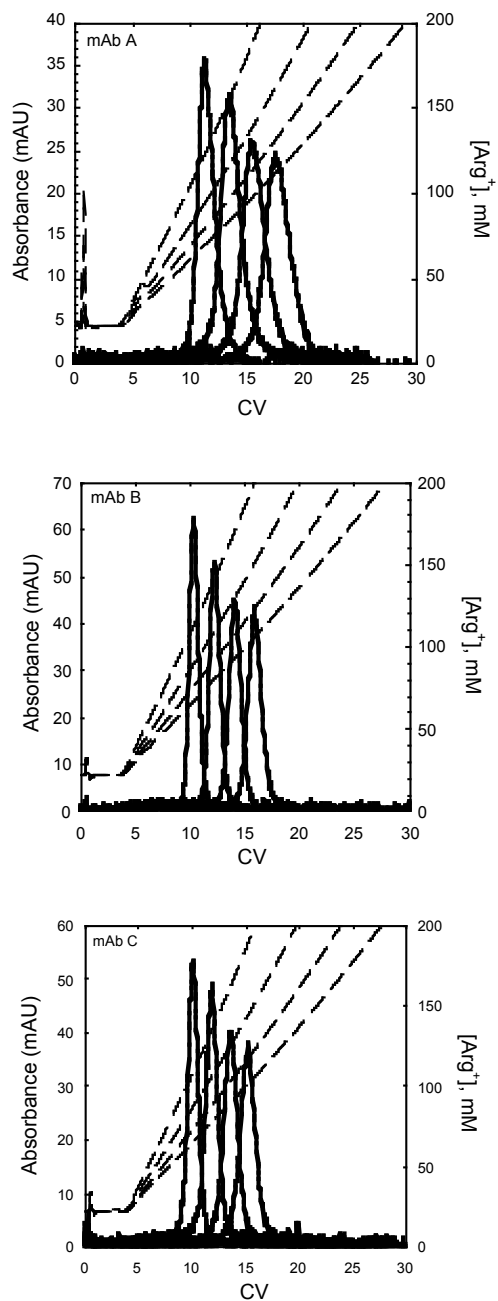
Figure 4.7f. Linear gradient elution (LGE) chromatograms obtained for POROS 50HS for mAb A, mAb B, and mAb C at different gradient slopes. The mobile phase was 20 mM arginine acetate at pH 7 with a final arginine concentration of 250 mM. The gradient durations were 15, 20, 25, and 30 column volumes.
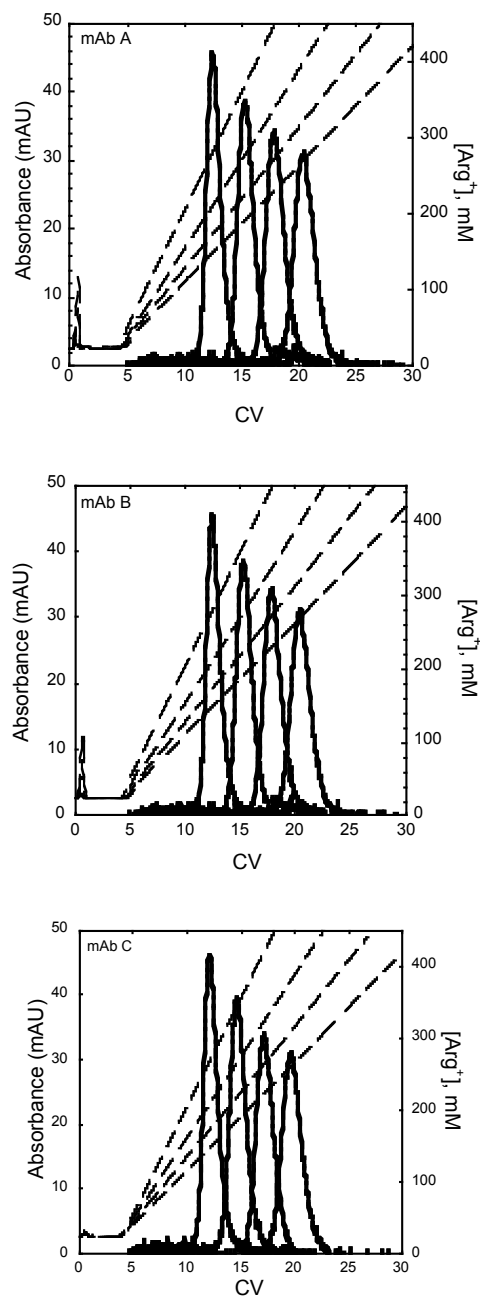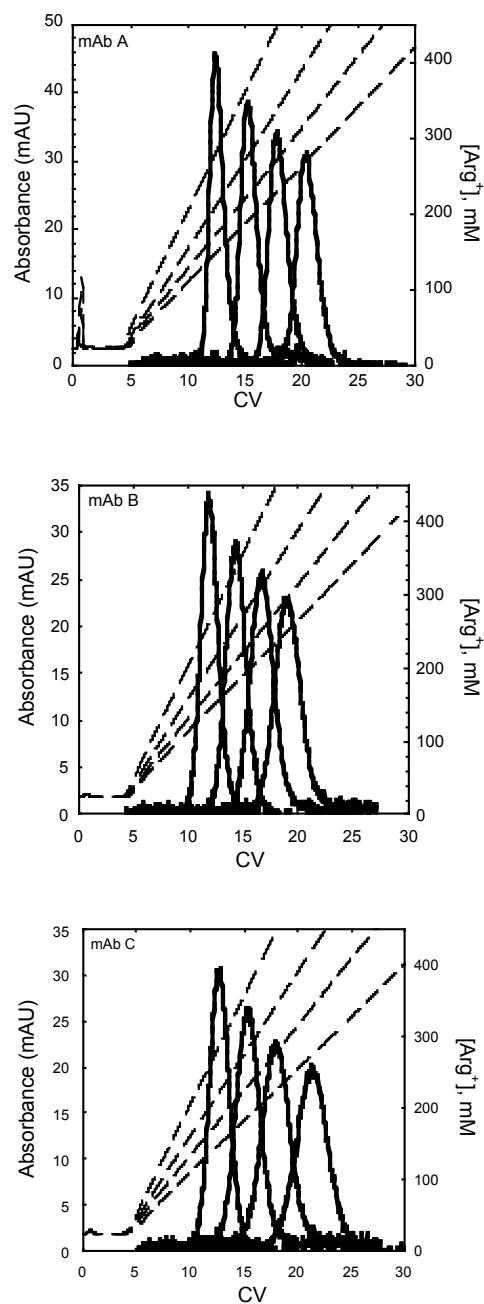
Figure 4.7g. Linear gradient elution (LGE) chromatograms obtained for UNOsphere Rapid S for mAb A, mAb B, and mAb C at different gradient slopes. The mobile phase was 20 mM arginine acetate at pH 5 with a final arginine concentration of 488 mM. The gradient durations were 15, 20, 25, and 30 column volumes.
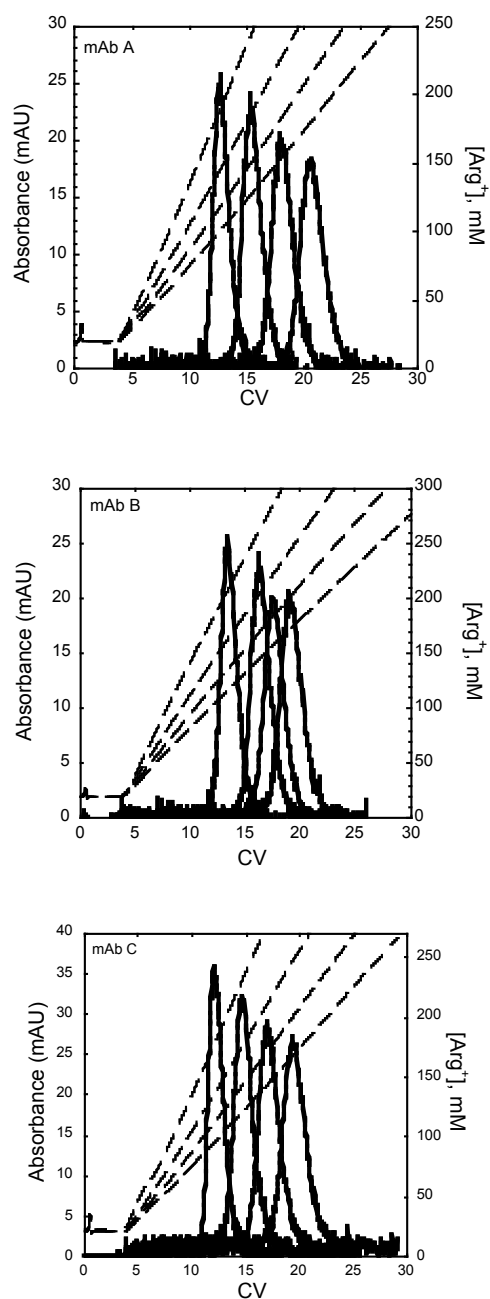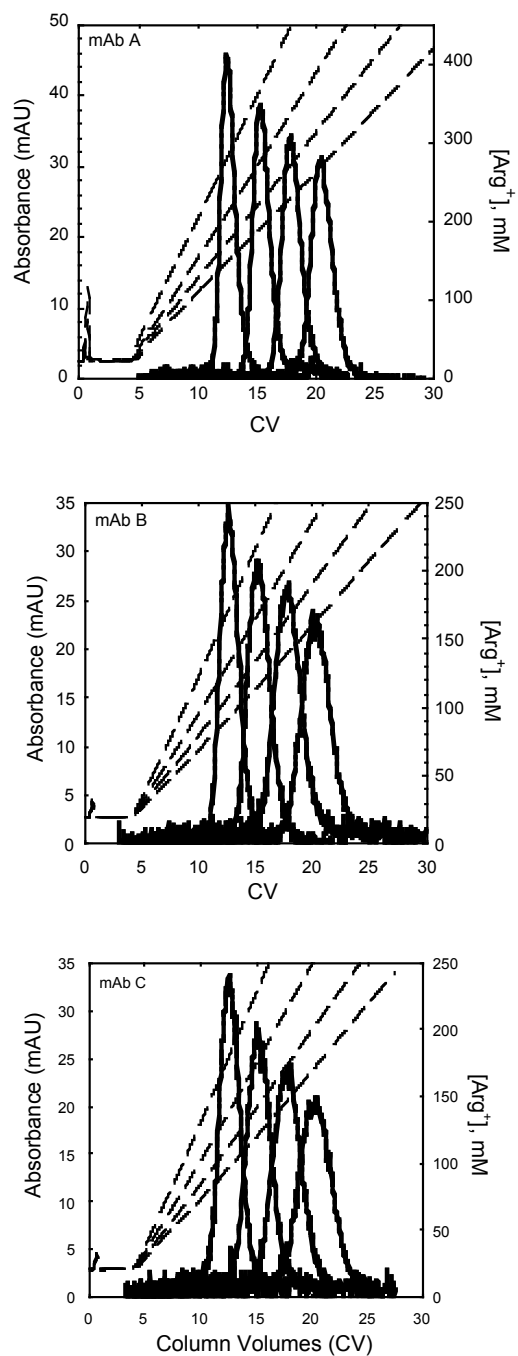
Figure 4.7h. Linear gradient elution (LGE) chromatograms obtained for UNOsphere Rapid S for mAb A, mAb B, and mAb C at different gradient slopes. The mobile phase was 20 mM arginine MES at pH 6 with a final arginine concentration of 300 mM. The gradient durations were 15, 20, 25, and 30 column volumes.
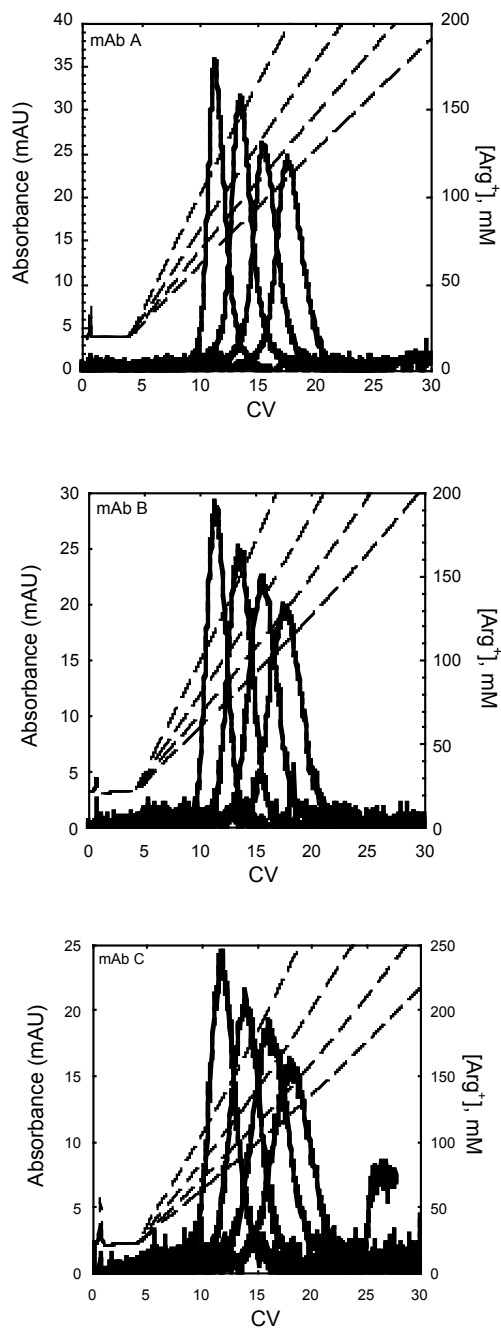
Figure 4.7i. Linear gradient elution (LGE) chromatograms obtained for UNOsphere Rapid S for mAb A, mAb B, and mAb C at different gradient slopes. The mobile phase was 20 mM arginine MES at pH 7 with a final arginine concentration of 250 mM. The gradient durations were 15, 20, 25, and 30 column volumes.

Table 4.4. Retention parameters for mAb A, B, and C at pH 5, 6 and 7 for Nuvia S, POROS 50HS, and UNOsphere Rapid S.

Resin	pH	mAb	Effective Charge, z_P	Affinity Parameter, A
Nuvia S	5	A	16.0±1.0	3.26×10^{39}
		B	16.3±1.4	5.28×10^{39}
		C	17.6±1.2	1.11×10^{43}
	6	A	11.4±0.7	2.70×10^{26}
		B	12.9±0.4	5.01×10^{29}
		C	13.0±0.7	4.10×10^{29}
	7	A	9.6±0.4	3.88×10^{20}
		B	11.7±0.9	3.88×10^{24}
		C	10.5±0.5	5.83×10^{21}
UNOsphere Rapid S	5	A	15.5±0.9	3.24×10^{38}
		B	16.8±1.5	6.26×10^{40}
		C	17.7±0.5	4.36×10^{43}
	6	A	11.4±0.7	3.97×10^{26}
		B	12.3±0.9	7.54×10^{27}
		C	13.3±0.6	1.94×10^{30}
	7	A	9.3±0.3	2.07×10^{21}
		B	11.1±0.5	2.11×10^{23}
		C	10.8±0.2	1.63×10^{23}
POROS 50HS	5	A	16.0±1.0	3.26×10^{39}
		B	16.5±1.0	1.07×10^{40}
		C	16.9±0.9	2.79×10^{41}
	6	A	11.1±0.6	7.46×10^{25}
		B	13.0±0.3	4.00×10^{29}
		C	13.7±0.5	1.01×10^{31}
	7	A	9.6±0.3	1.82×10^{21}
		B	11.1±0.3	1.50×10^{23}
		C	10.2±0.4	1.47×10^{21}

Figures 4.8a, b, and c show the calculated retention factors at pH 5, 6 and 7 for Nuvia, POROS, and UNOsphere. Retention of the three mAbs appears to be very similar to that obtained with sodium indicating for that these conditions, the mAbs interacted similarly with the resins regardless of the counterion used.

4.3 Protein Transport

4.3.1 Non-Binding conditions

The effective diffusivity of mAb A on POROS, UNOsphere, and Nuvia resins was obtained under non-binding conditions. Figure 4.9 shows the elution chromatograms and van Deemter plot. The elution peaks for both POROS and UNOsphere eluted at column volumes much larger than the extraparticle porosity, ε, and become broader and more skewed as the flow rate is increased indicating that the protein diffused into the resin pores. The Nuvia peaks, on the other hand, elute at CV values close to the extra particle porosity. This result suggests that the mAb molecules are excluded to a large extent from this resin for these conditions. The van Deemter plot, Fig. 4.9d, shows a linear relationship between h and v' for POROS and UNOsphere suggesting that mass transfer is limiting. For Nuvia however, h is essentially independent of v' indicating the a term in the van Deemter equation (eq. 3.1) is dominant and that mass transfer does not play a significant role. Based on eq. 3.1, the results for UNOsphere give $D_e/D_o=0.15\pm0.02$ or $D_e=(7.5\pm1.0)\mathrm{x}10^{-8}$ cm^2/s using the estimated free solution diffusivity of the mAb A. $D_o=5\mathrm{x}10^{-7}$ cm^2/s. A similar result is obtained for POROS with $D_e/D_o=(0.13\pm0.02)$ and $D_e=(6.5\pm1.0)\mathrm{x}10^{-8}$ cm^2/s. The effective diffusivity for Nuvia could not be determined from these experiments because the reduced HETP appeared constant with respect to flow rate.
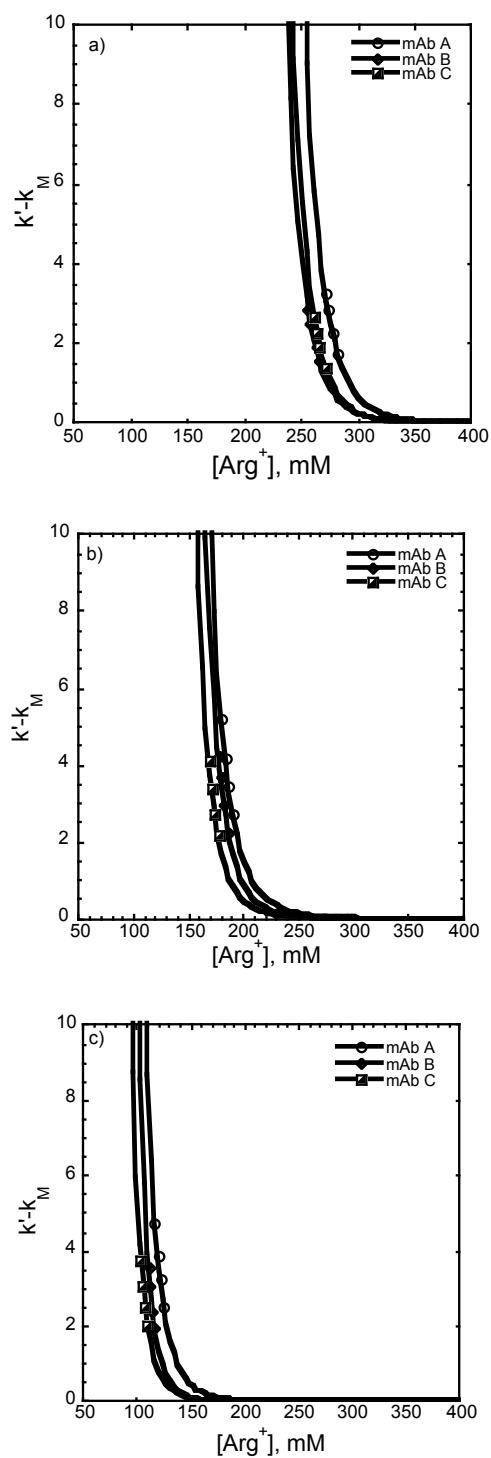
Figure 4.8a. Retention factors of mAb A, B, and C at (A) pH 5, (B) pH 6, and (C) pH 7 on Nuvia S.
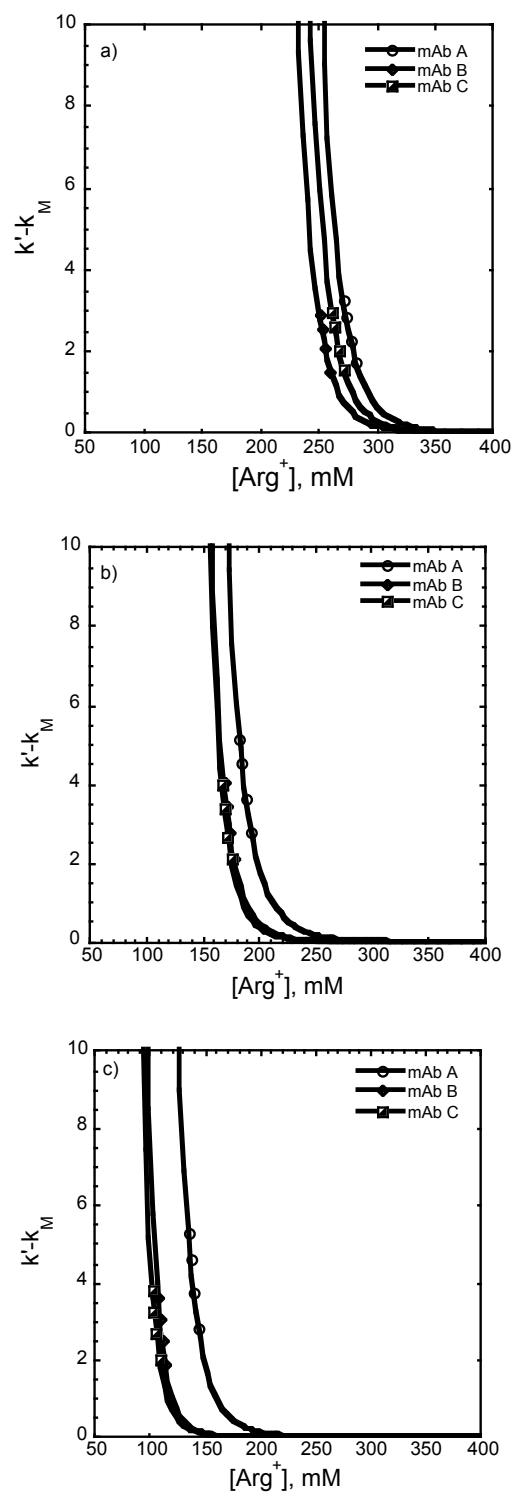
Figure 4.8b. Retention factors of mAb A, B, and C at (A) pH 5, (B) pH 6, and (C) pH 7 on POROS 50HS.
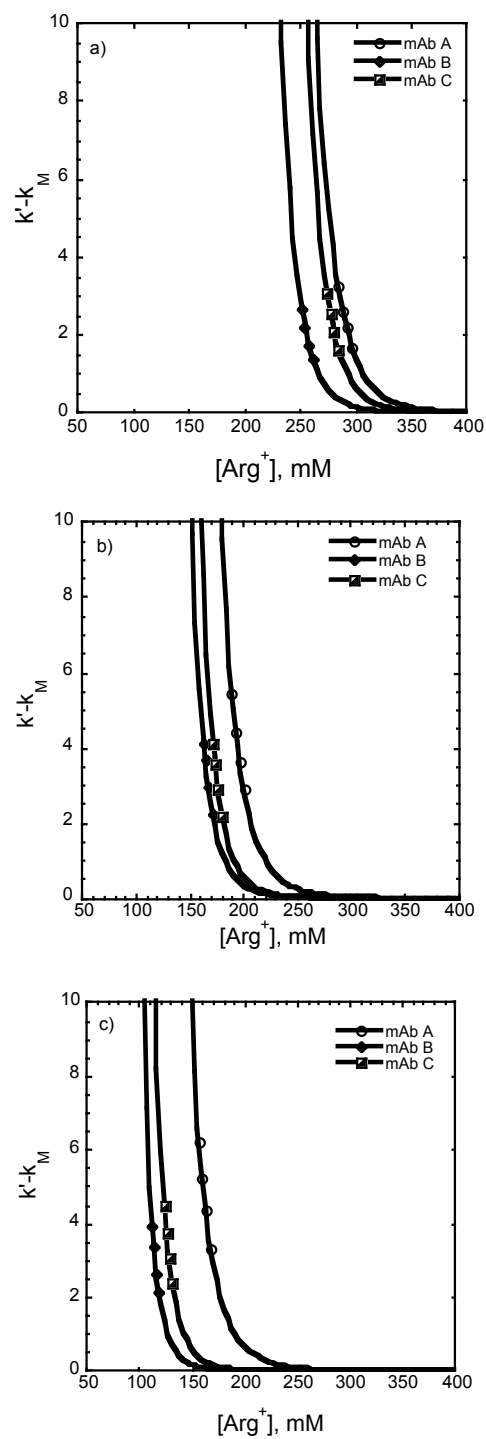
Figure 4.8c. Retention factors of mAb A, B, and C at (A) pH 5, (B) pH 6, and (C) pH 7 on UNOsphere Rapid S.
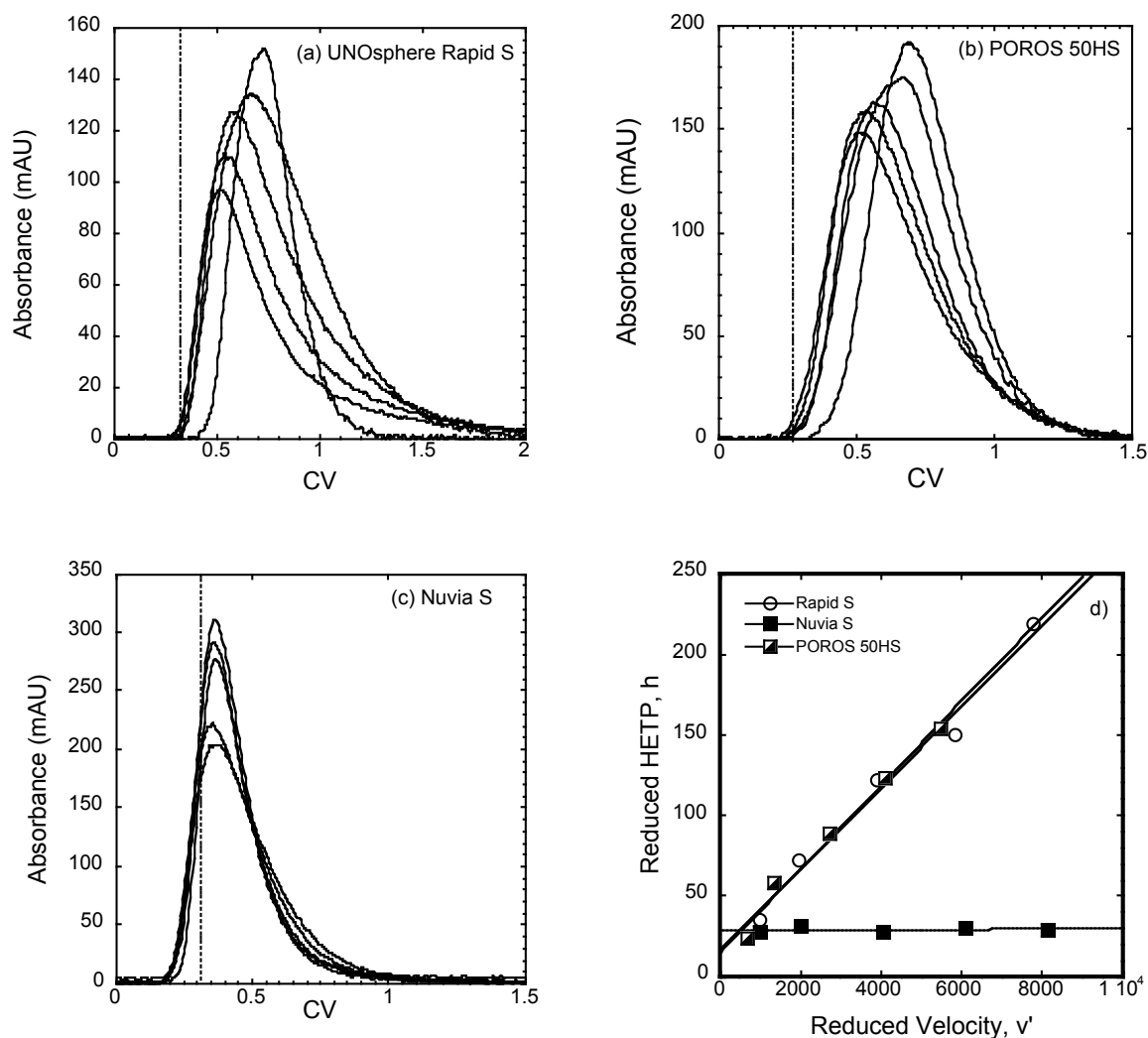
Figure 4.9. Isocratic pulse response peaks obtained under nonbinding conditions for mAb A in 1 M NaCl (a-c) and dimensionless van Deemter curves (d). Mobile phase superficial velocities for the curves shown in a-c were 0.65, 1.3, 2.6, 3.9, and 5.2 cm/min for UNOsphere Rapid S, 0.76, 1.5, 3.1, 4.6, 6.1 cm/min for POROS 50HS, and 0.73, 1.5, 2.9, 4.4, and 5.9 cm/min for Nuvia S, respectively. Vertical dashed lines in a-c indicate $CV = \varepsilon$.

4.3.2 Linear gradient elution with varying flow

Figure 4.10 shows the gradient elution chromatograms obtained at different flow rates and the corresponding van Deemter plot for mAb A. The elution peaks obtained with each resin are centered at the same CV, but become broader and more skewed as the flow rate is increased. UNOsphere had the broadest peaks and the most pronounced effect of flow rate. Nuvia S, on the other hand, showed the most asymmetry, which may be due to the polymeric surface extenders present in this resin. The HETP was calculated according to the following equation:

$$H = \frac{1}{16}\left(\frac{W}{V_R}\right)^2 d_p \qquad\qquad (4.3)$$

where W is the baseline peak width in volume units, d_p is the particle diameter, and V_R is the retention volume calculated for a peak eluted isocratically at $C_B = C_B^R$ according to:

$$V_R = \varepsilon V_c[1 + k'(C_B^R)] \qquad\qquad (4.4)$$

where Vc is the column volume and $C_B^R = [\gamma A(z_P + 1)]^{1/z_P + 1}$, which is obtained from eq. 4.2. Note that the peak compression factor (Carta and Jungbauer, 2010) was omitted in this calculation since its values are uncertain and the gradients used were fairly shallow indicating that the peak compression factors would be close to unity anyhow.

According to theory the reduced HETP, $h=H/d_p$ is related to v' by the following equation:
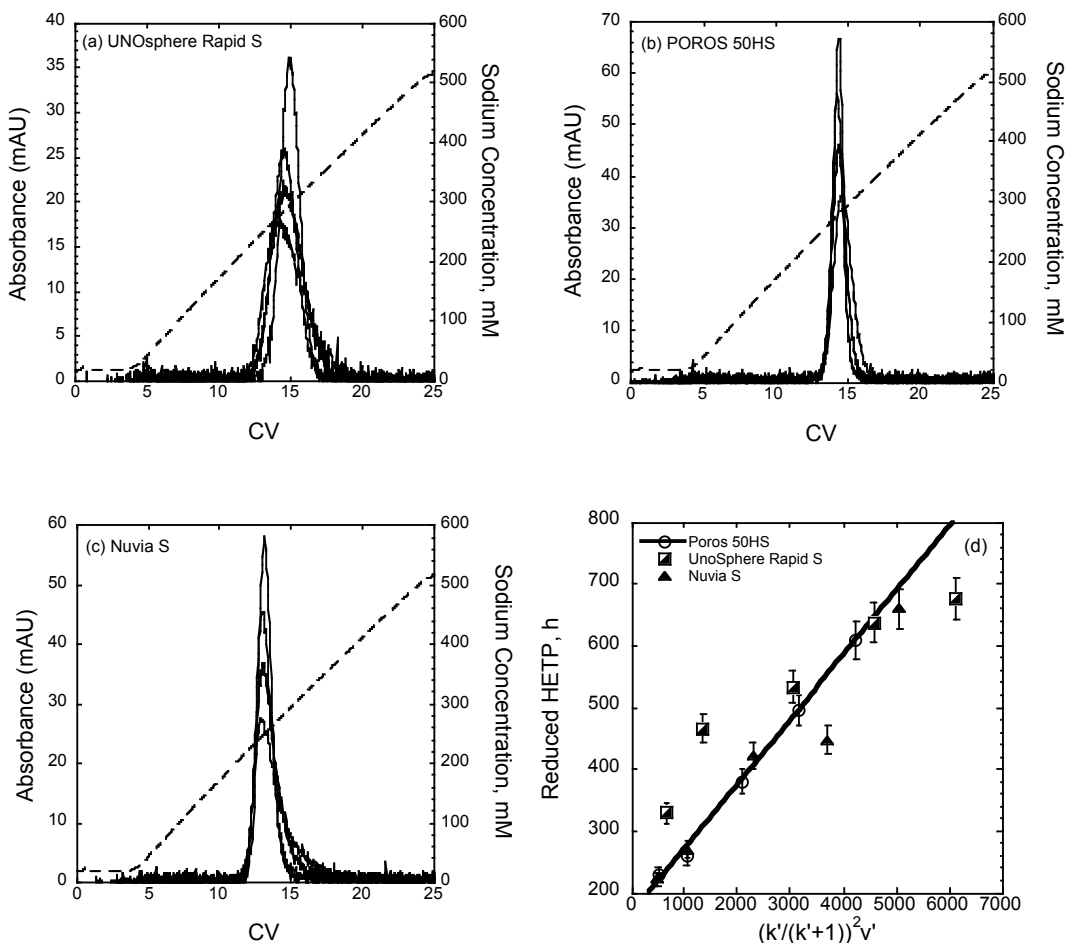
Figure 4.10. LGE chromatograms (a-c) and dimensionless van Deemter curves (d) for mAb A. Mobile phase superficial velocities were 0.65, 1.3, 2.6, 3.9, and 5.2 cm/min for UNOsphere, 0.76, 1.5, 3.1, 4.6, 6.1 cm/min for POROS, and 0.73, 1.5, 2.9, 4.4, and 5.9 cm/min for Nuvia, respectively. The mobile phase was 20 mM sodium acetate at pH 5 with a final sodium chloride concentration of 500 mM. The gradient duration was 20 column volumes.

$$h \cong a + \frac{1}{30}\frac{\varepsilon}{1-\varepsilon}\left(\frac{k'}{k'+1}\right)^2 \frac{D_o}{D_e}v' \qquad (4.5)$$

Accordingly, a plot of $\left[k'/(1+k')\right]^2 v'$ should be linear with a slope equal to. As seen in the data are reasonably well correlated by a straight line indicating that all these resins have similar D_o/D_e values.

Figure 4.11, compares the results obtained from the LGE experiments with those obtained for non-binding conditions. Although the scatter is large, there is general agreement between isocratic and LGE results for the macroporous resins UNOsphere and POROS. There is no such agreement however for Nuvia since this resin excludes the mAb under non-binding conditions resulting in a constant value of h.

4.4. Properties of Protein Aggregates

4.4.1. Preparation of aggregates

The formation, size, and stability of aggregates generated from mAb C were examined using size exclusion chromatography (SEC) and dynamic light scattering (DLS). Table 4.5 illustrates the course of aggregation of mAb C over time. The initial radius of 5nm is consistent with the estimates for a 150 kDa globular protein based on the correlations presented by Tyn and Gusek (1990). Increasing the time spent at this pH increases the apparent hydrodynamic radius indicating that aggregates are formed. Figure 4.12 shows the SEC chromatograms obtained for pure mAb C and for the aggregated mAb C solution after 48 hours and a comparison of the aggregate sample retention with known standards. As seen in this figure, two peaks are present at 48 hours, one with the same elution volume as the pure mAb and the other eluting earlier, consistent with a
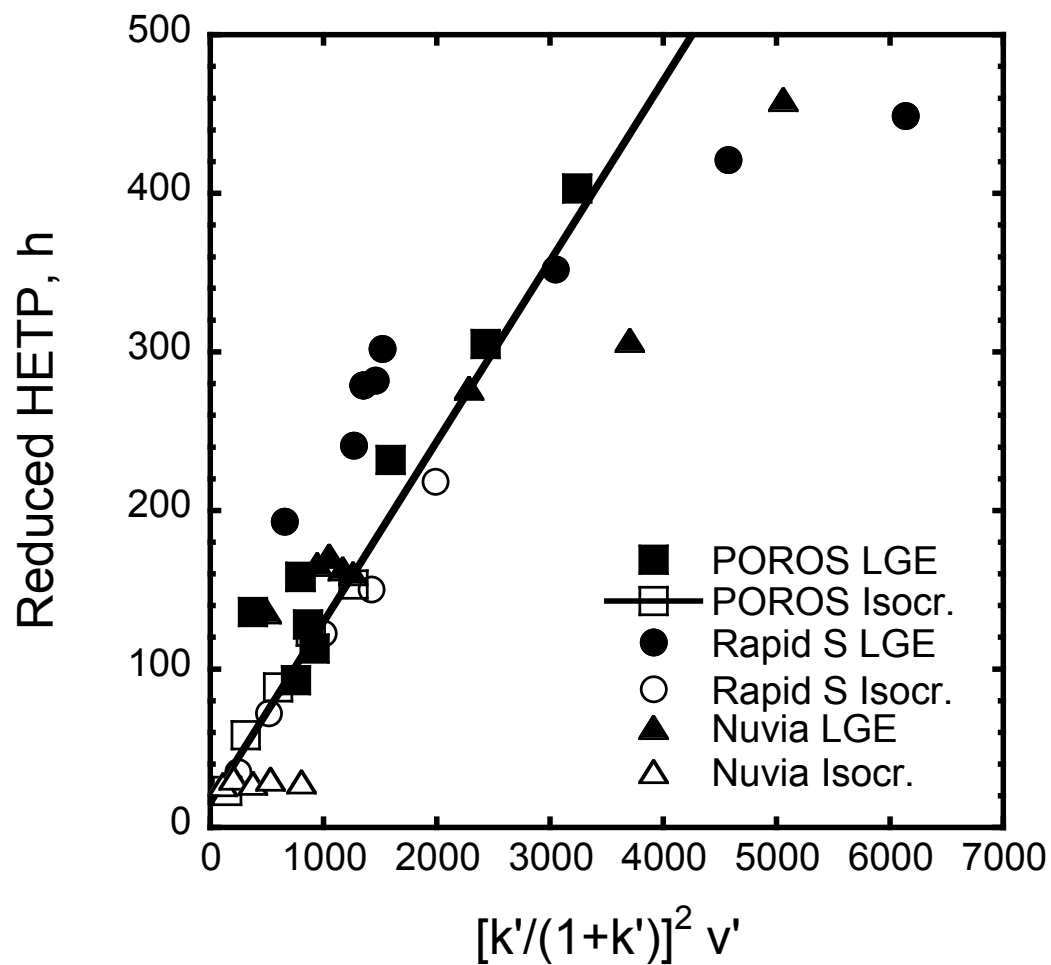
Figure 4.11. Dimensionless HETP for LGE and non-binding condition experiments based on mAb A results.

Table 4.5. Average apparent hydrodynamic radius of mAb C held in a pH 2.8 solution according to the procedure described in Section 3.2.6.1

Time(h)	Hydrodynamic Radius (nm)
1	5.0±0.2
3	5.2±0.1
6	6.3±0.3
24	6.6±0.2
48	7.2±0.4

larger size. By comparing the areas of the aggregate and monomer peaks, the 48 hour sample

contains approximately 40% aggregates. By comparison with the standards show in Fig. 4.12b the

hydrodynamic radii corresponding to the two peaks are 4.9 and 7.3 nm, respectively.

Figure 4.13 shows the same SEC analysis of the 48 hour sample as in Fig. 4.12 but with in-

line DLS and UV detection. Note that in this case, the early eluting peaks, corresponding to the

aggregates is much taller as the photon count rate is very sensitive to molecular size. Accordingly,

what seemed like a smaller shoulder to the left of the early eluting peak detected by UV is now a

clearly discernable peak. The hydrodynamic radii corresponding to the three peak maxima are

summarized in Table 4.6. The value obtained for peak 3 is the same as that obtained for the pure

mAb. The values of peak 1 and 2 are consistent with the aggregate size based on the elution of

protein standards (Fig 4.12a) and with the apparent radius determined by DLS for the 48 hour

monomer-aggregate mixture.

4.4.2 Aggregate LGE

4.4.2.1 pH effect

LGE experiments were conducted at different pH values using the 48 hour aggregated

mAb C sample and the results are shown in Fig 4.14. At least two major peaks are discernable

for both resins and at both pH values. The early eluting peak elutes at the same CV as pure mAb

in monomer form. The later eluting peak is believed to be mAb C aggregates. The results show

only modest resolution of monomer and aggregate for Nuvia at pH 5. The resolution improves

slightly at pH 7 with a more apparent separation of peaks but the overall resolution is still modest

when compared to the
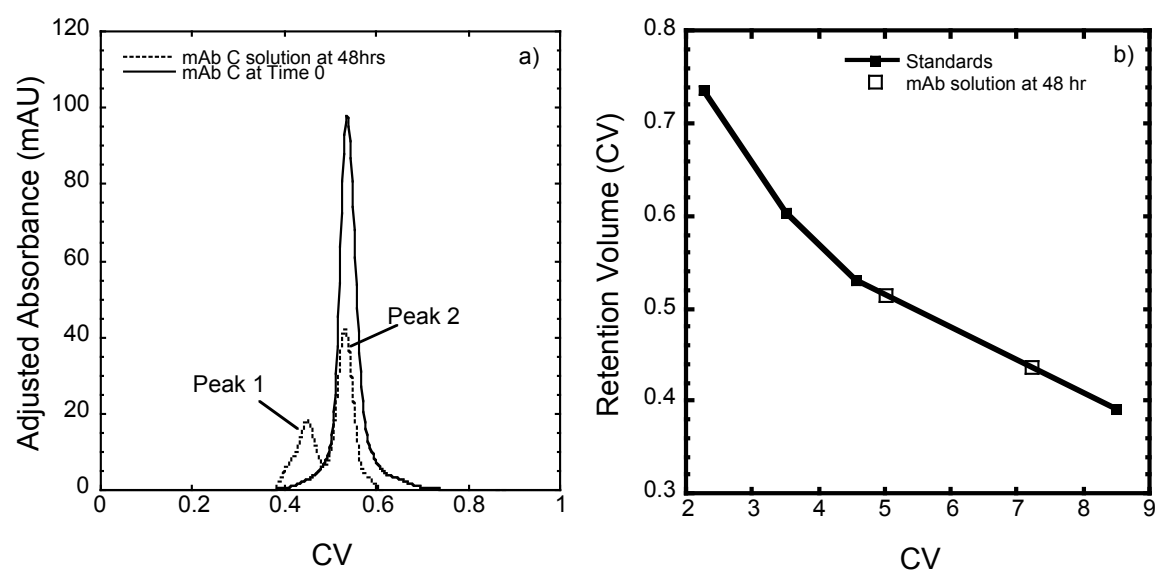
Figure 4.12. SEC chromatograms of pure mAb C and mAb C solution after 48 hours at pH 2.8

(a) and comparison of retention volume with hydrodynamic radii of protein standards (b).
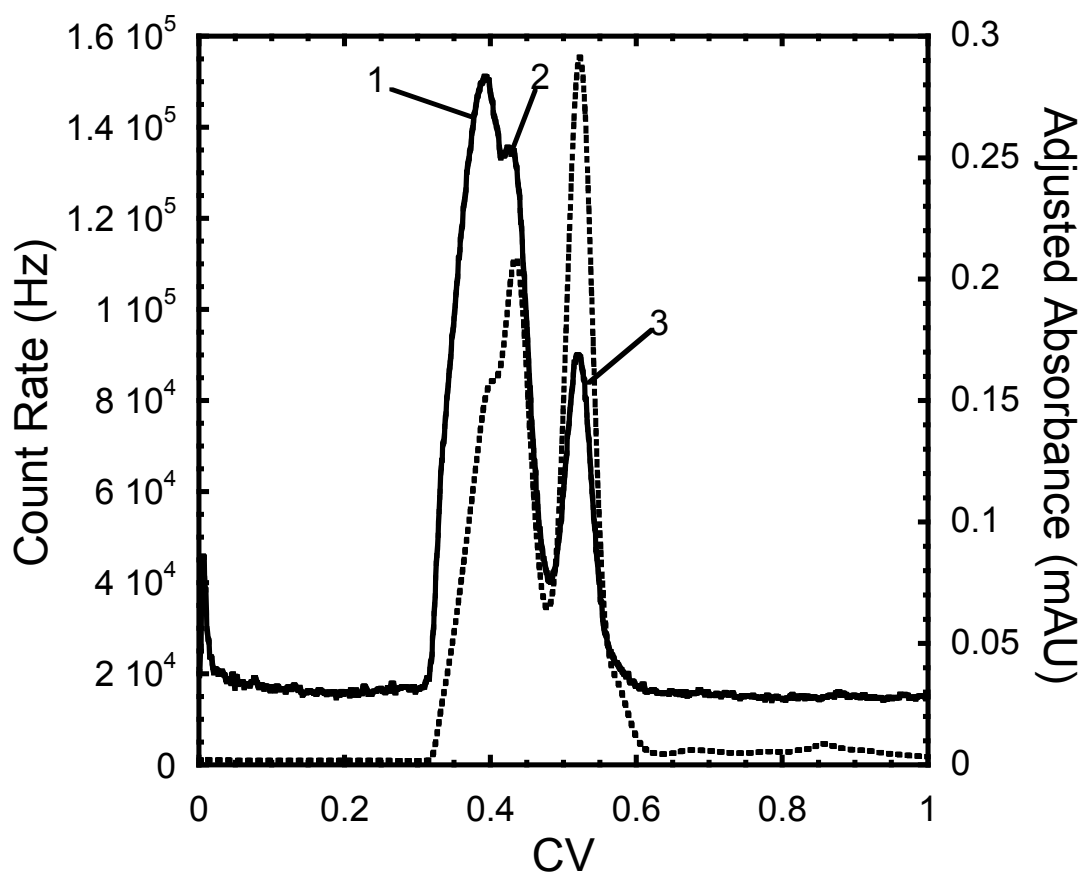
Figure 4.13. SEC separation of mAb C solution after 48hrs at pH 2.8, detected with in-line DLS detector (solid line) and UV detector (dotted line).

Table 4.6. Hydrodynamic radius determined by in-line DLS of mAb C solution separated by SEC (Fig. 4.13)

Peak	r_h (nm)
1	8.3±0.1
2	7.5±0.1
3	5.0±0.1
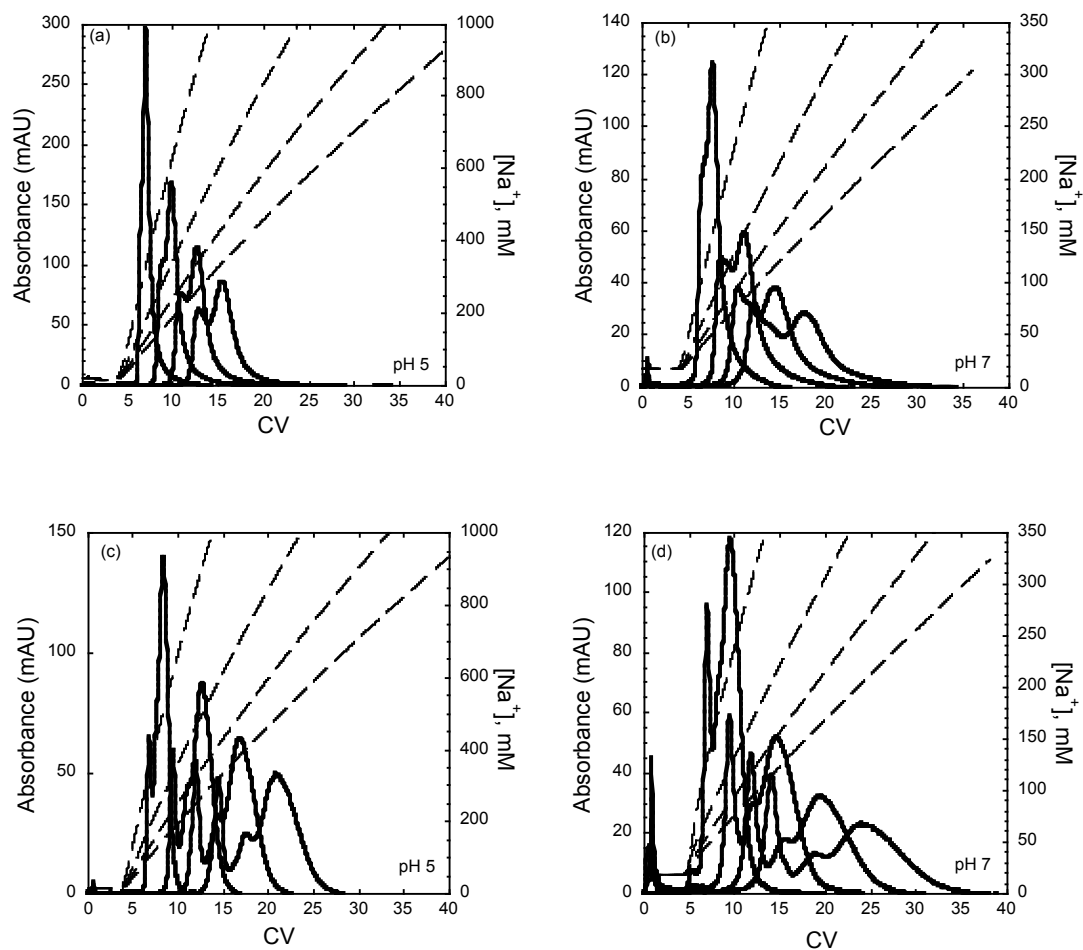
Figure

4.14. LGE chromatograms of the 48 hour aggregated mAb C sample for Nuvia S (a, b), and POROS 50HS (c, d) at pH 5 and 7. Gradient durations were 10, 20, 30 and 40 column volumes.

resolution obtained with POROS (Fig 4.14 c and d). The chromatograms for POROS display almost complete resolution of the early eluting monomer peak from the later eluting aggregate peak. The percentage of aggregate present in the LGE chromatograms appears to be much higher than in the SEC chromatograms in Section 4.4.1. The increase in aggregate may be related to unfolded monomers in solution which aggregate during interaction with resin, or by the high salt concentration used for elution which may cause further aggregation.

The regressed values of z_P and A determined (as described previously for the pure monomer LGE experiments) for the early and late eluting peaks are given in Tables 4.5 and 4.6. The retention parameters obtained for the early eluting peak are consistent with the values obtained for the pure monomer experiments described in Section 4.2.2. The regressed parameters obtained for the late eluting peak show an effective charge approximately twice that of the monomer peak and a larger affinity parameter.

The calculated retention factors of the monomers and aggregates for Nuvia and POROS are shown in Figs 4.15 and 4.16. At pH 5, the difference between monomers and the mAb C aggregates is very large for both POROS and Nuvia suggesting that this condition could be used for a robust separation of aggregates from a mAb mixture without resolving the monomers. At pH 7, however, the difference between mAb A and the mAb C aggregates becomes much smaller making this pH less favorable. The same trend holds true for Nuvia. However, the difference between monomer and aggregate is much smaller than that of POROS. From the chromatograms as well as the retention plots, it appears that POROS is better at separating the monomers from the aggregates.

Table 4.8. Retention parameters for peak 1 of mAb C aggregate solution obtained from LGE experiments

Resin	pH	Effective Charge, z_P	Affinity Coeffecient, A
Nuvia S	5	17.3 ±0.6	2.29×10^{42}
	7	10.6± 0.4	2.64×10^{21}
POROS 50HS	5	17.4± 1.5	1.02×10^{44}
	7	10.1± 0.5	2.45×10^{21}

Table 4.7. Retention parameters for the second major peak of the mAb C aggregate solution obtained from LGE experiments

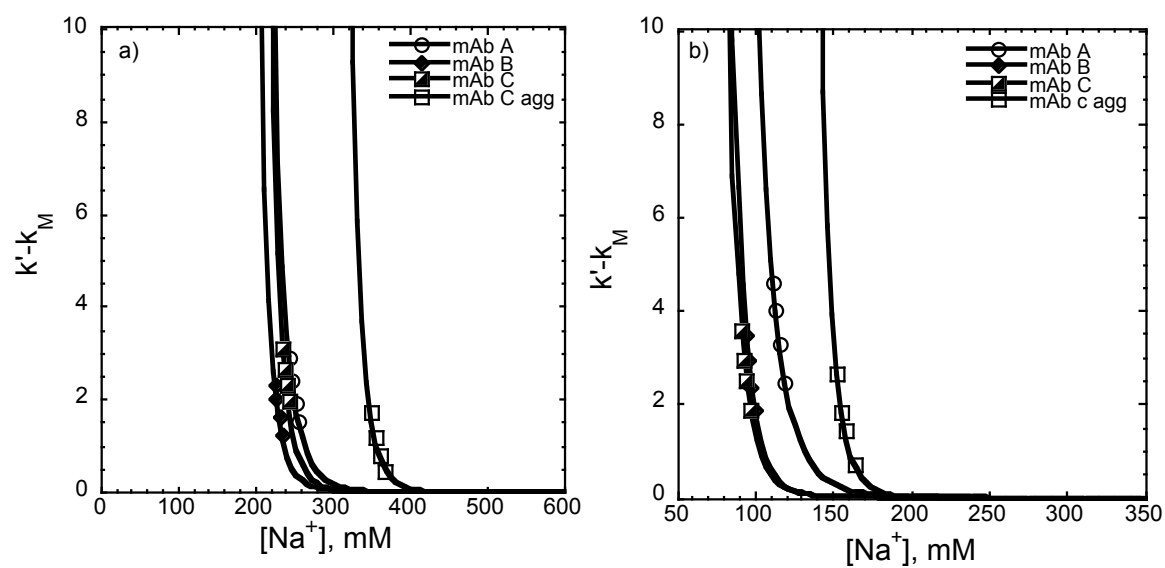| Resin	pH	Effective Charge, z_P	Affinity Coefficient, A
Nuvia S	5	27±2	4.74×10^{73}
	7	20±2	2.07×10^{46}
POROS 50HS	5	25±2	3.76×10^{64}
	7	19±2	7.32×10^{42}

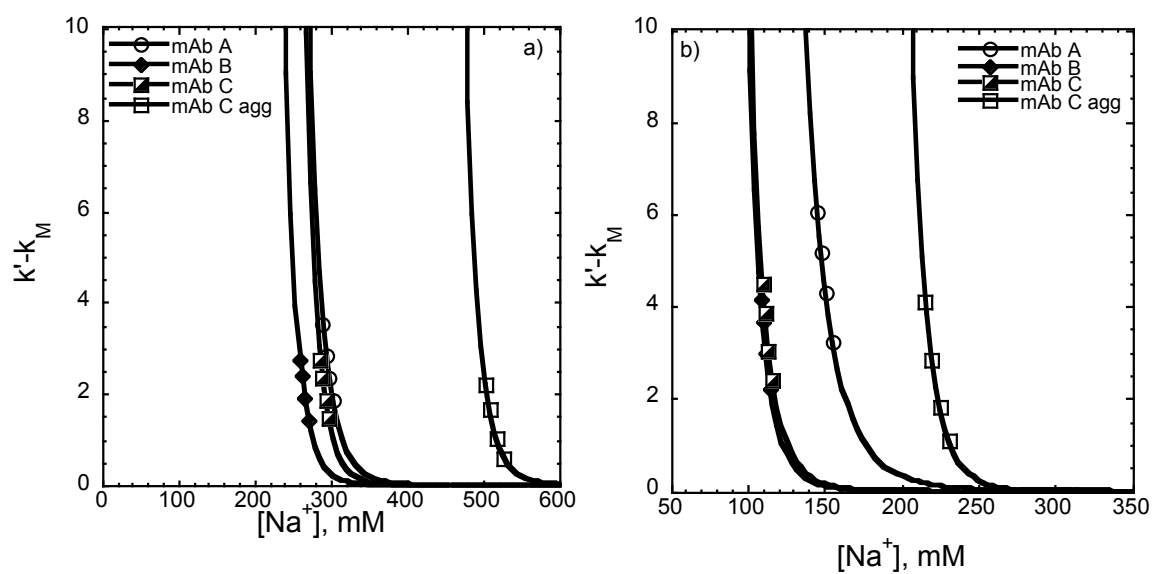Figure 4.15. Protein retention plots of mAb A, B, C and C aggregates at (A) pH 5, and (B) pH 7 on Nuvia S.

Figure 4.16. Protein retention plots of mAb A, B, C and C aggregates at (A) pH 5, and (B) pH 7 on POROS 50HS.

4.4.2.3 Step elution

The separation of the three mAbs from the mAb C aggregates was tested using a salt step on a POROS 50HS column. A solution containing equal part mixture of all three mAbs at total protein concentration of 3 g/L was spiked with a 65/35 mixture of mAb C monomer and aggregate so that the final solution was 91% monomer and 9% aggregate. 300 micrograms was then injected to the column and subjected to 2 concentration steps. The first step was to increase the sodium concentration from 20 to 350 mM and the second to increase from 350 to 1020 mM these values were selected based on Fig. 4.16a so that the first step would only elute the monomers while the second step would elute the mAb C aggregate.

Figure 4.17 shows the chromatogram obtained with these steps. A large peak, believed to correspond to the monomers, appears upon the first step with another smaller peak, believed to be comprised of the mAb C aggregate, elutes with the second step. The area of the second peak is 7.6% of that of the first peak. The molecular size corresponding to each peak was also determined by in-line DLS. For this experiment, a sample was prepared containing 2 g/L of an equal part mixture of each monomer and spiked with a 60/40 mixture of mAb C monomer and aggregate so that the final percentage of aggregate in the solution was 40% in order to obtain more accurate results from the DLS instrument. The results are shown in Fig. 4.18 and Table 4.9. A preliminary conclusion is that at low c-aggregate loads the late eluting peak is within 1.6% of the percentage of c-aggregates injected to the column. However, at higher protein loads and percentage of c aggregate, the late eluting peak contains a significantly greater percentage of high molecular weight (HMW) species than the injected sample. The size determined by in-line DLS, for this peak is also significantly larger than for the HMW species in the injected sample. One possibility is that higher ordered species are formed in either the column loading or elution. Nevertheless, the step elution
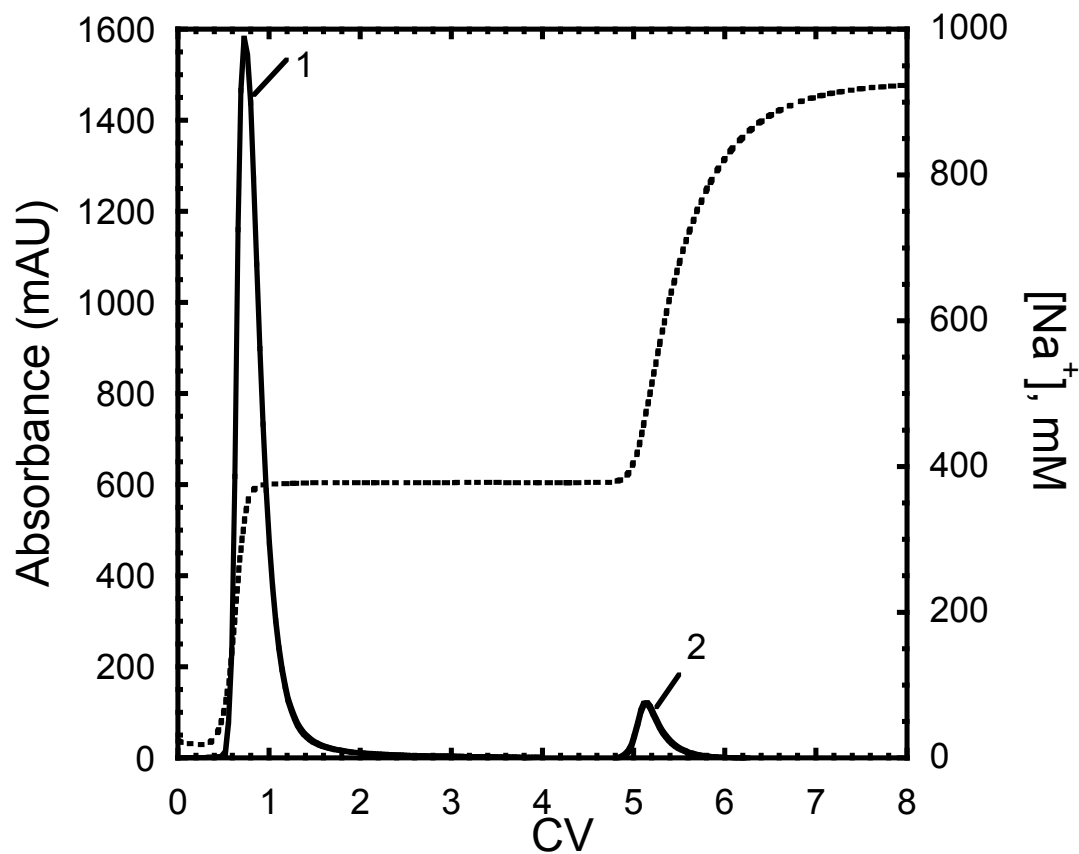
Figure 4.17. Step elution chromatogram of mAbs A,B, C and mAb C aggregates performed on

POROS 50HS at pH 5. The concentration of the first step was 350 mM and the second was 1020

mM. The injected protein load was 100 µL of a 3 g/L solution
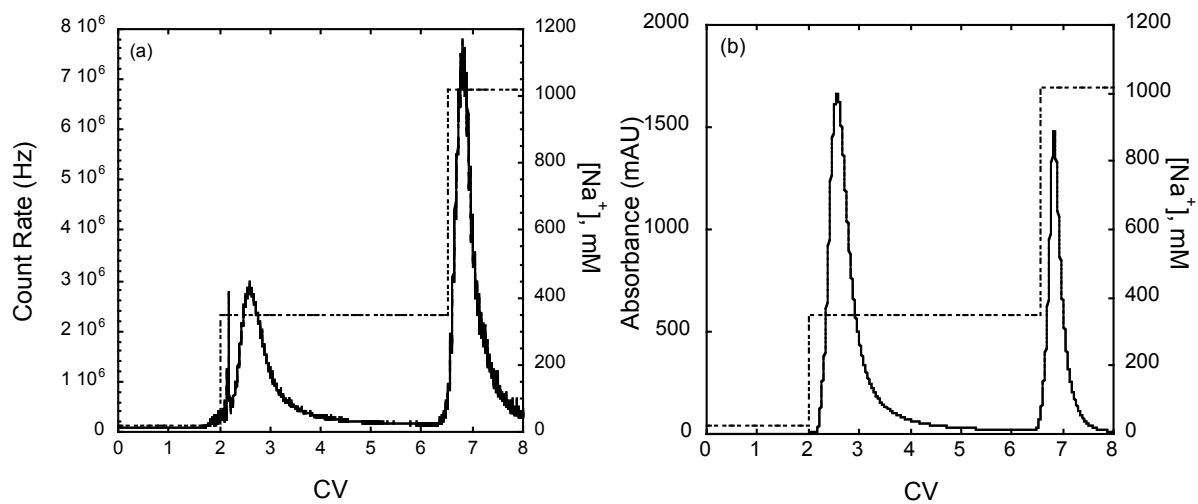
Figure 4.18. Step separation of mAb A, B, and C from mAb C aggregates for POROS 50HS detected with in-line DLS (a) and UV (b). The dashed line indicates the theoretical sodium concentration. The protein load was 300 µL of 3.8 g/L solution.

Table 4.9. Step elution conditions and results

Run	% of HMW in C aggregated sample	Protein concentration in injected sample	Protein load (mg)	% HMW in injected sample	% HMW in late eluting peak	r_h (nm) of early eluting peak	r_h (nm) of late eluting peak
1	35.4	0.75 mg A /mL 0.75 mg B/mL 1.23 mg C/mL 0.27 mg C agg/mL	0.3	9.0%	7.6%	-	-
2	52.7	0.95 mg A /mL 0.95 mg B/mL 0.97 mg C/mL 0.90 mg C agg/mL	1.13	24%	32± 2%	5.6±0.2	14±0.5
3	52.7	1.61 mg C/mL 1.80 mg C agg/mL	1.02	53%	68%	-	-

results demonstrate the ability to separate the HMW species from the monomers without resolving the individual monomer constituents.

5 Conclusion:

An investigation was conducted to determine the possibility of the purification of recombinant polyclonal antibodies by ion exchange chromatography. Both the single component equilibrium and transport kinetics of the purified mAbs as well as the aggregates were considered. Important conclusions regarding the effect of pH, resin properties, and counterion type were determined and are summarized below. The results of this work offer valuable insight into monoclonal antibody and monoclonal antibody aggregate behavior as well as their separation.

5.1 Single component LGE

The equilibrium parameters for three different monoclonal antibodies were determined by ion exchange chromatography. The three different commercial strong cation exchangers, UNOsphere Rapid S, Nuvia S and POROS 50HS were examined to determine the ideal properties for co-elution of the mAbs. Two different counterions, sodium and arginine, were tested as well at three different pH values. The results of these experiments showed that counterion type had little effect on the overall behavior of each mAb, and therefore co-elution would be no more likely with one counterion as opposed to the other. The pH of the system had a much larger effect, as it affected the retention of each mAb differently. From these experiments, it was determined that based on the retention and resolution of the mAbs, Nuvia S and POROS 50HS operated at pH 5 and 7 with sodium as the counterion offered the best opportunity for co-elution.

5.2 Protein Transport

Chromatographic analyses under non-binding and binding conditions were performed to study mass transfer kinetics of single component monoclonal antibodies. The results of the non-binding condtion experiments provided consistent results with previous findings by Tao et. al (2011) which found that mAb molecules can access the pores in the macroporous resins, POROS 50HS and UNOsphere Rapid S, but were almost completely excluded from the Nuvia S particles.

The experiments performed under operating conditions showed that the behavior of the monoclonal antibodies on all three resins was approximately the same as the behavior seen for the pore diffusion controlled resins under non-binding conditions. This result indicates that the dextran graphs in Nuvia S seem to have a negligible effect the mass transfer of the antibody molecules out of the resin.

5.3 Monoclonal antibody studies

The production and characterization of low pH monoclonal antibody aggregates was performed to determine the size, equilibrium parameters, and retention of the aggregates formed. Both batch mode dynamic light scattering as well as size exclusion chromatography were used to determine the overall extent of aggregation over time. The results showed increasing amounts of aggregate over time, with approximately a 50-50 mixture of aggregate to monomer after 48 hours. The size and order of the aggregates produced was determined by using inline dynamic light scattering experiments, the results of which showed the aggregates that were produced were likely in the range of tetramers and dimers. After the characterization of the aggregates, linear gradient elution experiments were performed on the aggregates using the conditions determined from the single component experiments. POROS 50HS showed much better resolution and selectivity than Nuvia S for the separation of aggregate from monomer. From the retention of the

aggregate and monomer, a concentration step was designed. The results of this step were then tested using inline dynamic light scattering which showed two elution peaks, the first containing only monomer and the second containing aggregate.

6. Recommendations:

6.1 rpAb purification model

This thesis provides a detailed investigation into the single component behavior of three antibodies and antibody aggregates which allowed for the prediction and separation of monomers from aggregates. Ideally, the prediction of the separation of recombinant polyclonal antibodies from their aggregates could be done without requiring an exhaustive study of the single component behavior of each individual mAb and aggregate component. The formation of a model based on the molecular properties of the antibodies and the chromatographic behavior of the mAb aggregates could drastically increase the rate at which a downstream purification process is developed for rpAbs.

As this study showed, there is only a small correlation between the antibody's pI and the chromatographic behavior. Using linear gradient elution experiments, the effective charge and affinity were able to be determined at a variety of conditions. It is hypothesized that a relationship between these variables and the molecular properties of the antibody could be formed. With this information it could be possible to determine the possibility of purification without fractionation during drug development. This could allow for simple manipulations in the early stage drug design with the downstream purification in mind.

Further investigation should be done to understand the behavior of the mAb aggregates on polymer grafted resins. Desorption experiments, both single and multicomponent, could be performed to better understand the elution behavior of the aggregates. These experiments would provide insight into the elution behavior of the aggregates, and could help determine if it is possible to separate the larger aggregates from the smaller monomers on these matrices.

Confocal scanning laser microscopy (CLSM) and stirred batch experiments could provide insight into this behavior.

A study of transport properties of the mAb aggregates is necessary in order to accurately model the adsorption kinetics and behavior of the mAb aggregates. As stated previously, mass transfer is often the limiting step in chromatographic processes. Non binding experiments and LGE experiments with varying flow rates should be performed. The information from these experiments could be utilized to determine the rate of mass transfer for the aggregates as well as the method of mass transfer.

The effect of load size should also be determined. In industrial applications, chromatographic processes are operated at high loading capacities to maximize productivity. In these situations, the resolution is dependent on the feed load. As a result it would be useful to examine the effect of the load size to determine the effect this has on the resolution and selectivity of the process.

7. References:

Applied BioSystems, Properties of POROS 50HS, Technical Bulletin, 2012..

Bio-Rad, Properties of UNOsphere Rapid S, Technical Bulletin, 2012.

Bio-Rad. Properties of Nuvia S, Technical Bulletin, 2012.

Bregenholt, S., Jensen, A., Lantto, J., Hyldig S., Haurum, J.S., Recombinant human polyclonal antibodies: A new class of therapeutic antibodies against viral infections. Current pharmaceutical design 12(2006) 15.

Brooks, C., Cramer, S., Steric mass-action ion exchange: Displacement profiles and induced salt gradients."AIChE Journal 12 (1992) 1969–1978.

Carta, G., a. R. Ubiera, and T. M. Pabst., Protein Mass Transfer Kinetics in Ion Exchange Media: Measurements and Interpretations. Che Eng & Tech., 28 (2005), 1252–1264.

Carta, G., Jungbauer, A., Protein Chromatography: Process Development and Scale-Up, Wiley, Weinheim, 2010.

Cussler, E.L., Diffusion: Mass Transfer in Fluid Systems, Cambridge University Press, New York, 1997.

Ejima, Daisuke, Kouhei Tsumoto, Harumi Fukada, Ryosuke Yumioka, Kazuo Nagase, Tsutomu Arakawa, and John S Philo. Effects of Acid Exposure on the Conformation , Stability , and Aggregation of Monoclonal Antibodies, 962 (2007) 954–962.

Forrer, Nicola, Alessandro Butté, and Massimo Morbidelli., Chromatographic behavior of a polyclonal antibody mixture on a strong cation exchanger column. Part I: Adsorption Characterization, J. Chromatogr. A,1214 (2008), 71–80.

Frandsen, T. P, Naested, H., Rasmussen, S.K., Hauptig, P.,Wiberg, F.C., Rasmussen,L. K., Jensen, A.M., Persson, P., Wikén, M. Engström, A., Jiang, Y., Thorpe, S.,J., Förberg, C., Tolstrup, A.B., Consistent manufacturing and quality control of a highly complex recombinant polyclonal antibody product for human therapeutic use, Biotech. Bioeng. 108 (2011): 2171–81.

Helfferich, F., *Ion Exchange*. New York: McGraw Hill. (1962).

LeVan, M.D., G.Carta, C.M. Yon. Adsorption and Ion Exchange, Perry's Chemical Engineers Handbook, 8th Edition, McGraw-Hill, New York, 2007.

Perez Almodovar, E. X., Glatz, B., Carta, G., Counterion effects on protein adsorption equilibrium and kinetics in polymer-grafted cation exchangers, J. Chromatogr. A., 1253 (2012), 83–93.

Shukla, A. A., Hinckley, P., Host Cell Protein Clearance During Protein A Chromatography : Development of an Improved Column Wash Step.(2008)

Tao, Y., Perez Almodovar, E.X., Carta, G., Ferreira,G., Robbins,D., Adsorption kinetics of deamidated antibody variants on macroporous and dextran-grafted cation exchangers. III. Microscopic studies, J. Chromatogr. A,1218 (2011) 8027–35.

Tyn M., Gusek T., Prediction of diffusion-coefficients of proteins," Biotechnol. Bioeng., 35 (1990) 327-338.

U.S. Department of Health and Human Services Food and Drug Administration Office of the Commissioner Office of Combination. Current Good Manufacturing Practice for Combination Products., Technical Bulletim, 2004.

Weaver, L.E., Carta, G., Protein Adsorption on Cation Exchangers : Comparison of Macroporous and Gel-Composite Media, 50 (1996) 342–355.

Yamamoto S, Nakanishi K, Mastuno R., Ion Exchange Chromatography of Proteins, New York, Dekker,1988.

Yamamoto, S., Plate height determination for gradient elution chromatography of proteins. Biotech. Bioeng, 48 (1995) 444–51.